Gabriel Barbosa Coutinho Freire de Souza

Application of a Soft Root Technique to the Welding of High Strength Steels (HSS)

School of Aerospace, Transport and Manufacturing
Welding Engineering

MSc
Academic Year: 2024–2025

Supervisor: Dr Supriyo Ganguly
Associate Supervisor: Dr Graeme Barritte
November 2025

School of Aerospace, Transport and Manufacturing
Welding Engineering

MSc

Academic Year: 2024–2025

Gabriel Barbosa Coutinho Freire de Souza

Application of a Soft Root Technique to the Welding of High Strength Steels (HSS)

Supervisor: Dr Supriyo Ganguly
Associate Supervisor: Dr Graeme Barritte
November 2025

This thesis is submitted in partial fulfilment of the requirements for the degree of MSc.

Academic Integrity Declaration

I declare that:

- the thesis submitted has been written by me alone.
- the thesis submitted has not been previously submitted to this university or any other.
- that all content, including primary and/or secondary data, is true to the best of my knowledge.
- that all quotations and references have been duly acknowledged according to the requirements of academic research.

I understand that to knowingly submit work in violation of the above statement will be considered by examiners as academic misconduct.

Abstract

The increasing use of High-Strength Steels (HSS) in structural applications poses significant challenges to welding, particularly in selecting compatible filler metals with the same level of strength and in reducing the likelihood of cold cracking. Among the strategies proposed to address these issues, the use of a "soft root", a root pass made with a lower-strength filler metal, has been studied.

This research investigates the effects of applying a soft root configuration in the welding of a HSS (S690). The study explores the use of two different filler metals: a lower-strength wire applied to the root and a higher-strength wire used in the fill and cap passes. The experimental set included tensile tests, Charpy impact tests, hardness surveys, Scanning Electron Microscopy (SEM), and metallographic analysis to evaluate joint performance.

The results indicate that the soft root configurations, even with mismatch ratios as low as 0.57, did not compromise mechanical integrity, reducing hardness and increasing ductility. Samples with a soft root did not behave as unmatched joints, outperforming the predictions of Eurocode 3 (EC3) curve. These findings support the strategy as a viable design alternative for welding HSS, especially in scenarios where matching or overmatching consumables and cold cracking are concerns. More research is recommended to unlock the full potential of this technique.

Keywords:
undermatched welds; soft root technique; HSS welding; weld metal mismatch; cold cracking mitigation; fracture toughness; S690 steel

Acknowledgements

The author expresses his deepest gratitude to his parents, Marcia and Helio, who have always gone above and beyond to ensure a quality education. Special thanks to his sister Erica for her unwavering friendship and to his wife Daniele for choosing to dream his dream alongside him.

This work is dedicated to his son Caio, as a reminder to never let anyone tell him that he is not capable of achieving something. Challenges are not obstacles. In fact, they are incentives to build bridges.

The author is also sincerely grateful to his supervisors, Dr. Supriyo Ganguly and Dr. Graeme Barritte and all other staff members for their valuable guidance, support, and for everything they have contributed throughout his time at Cranfield University.

Finally, the author would like to thank the Brazilian Navy for funding this research and supporting his stay in the United Kingdom. Technological sovereignty is a path to true independence.

Table of Contents

List of Figures

List of Tables

List of Abbreviations

BCC	Body Centre Cubic
BM	Base Metal
CE	Carbon Equivalent
CTOD	Crack Tip Opening Displacement
CP	Complex Phase
DP	Dual Phase
EBSD	Electron Backscatter Diffraction
EC3	Eurocode 3
EDS	Energy Dispersive Spectroscopy
FCAW	Flux Cored Arc Welding
FCW	Flux Cored Wire
HAZ	Heat-Affected Zone
HICC	Hydrogen Induced Cold Cracking
HSLA	High Strength Low Alloy
HSS	High Strength Steels
LBW	Laser Beam Welding
NDT	Non Destructive Test
PWHT	Post-Weld Heat Treatment
QT	Quenched and Tempered
SEM	Scanning Electron Microscopy
SRT	Soft Root Technique
TMCP	Thermo-Mechanically Controlled Processed
TRIP	Transformation-Induced Plasticity
UTS	Ultimate Tensile Strength
Y/T	Yield to Tensile ratio
WM	Weld Metal
WPQR	Welding Procedure Qualification Record

Chapter 1

Introduction

1.1 Overview

Engineering is constantly looking for ways to optimise solutions with the primary objective of reducing weight while maintaining the structural integrity of the components. In this context, High-Strength Steels (HSS) have emerged as an important material as they offer an excellent ratio between strength and weight reduction.

HSS has been increasingly used in a wide range of structural applications such as civil engineering, offshore, and the energy sector (1). In these contexts, HSS enables lighter and more efficient designs, as well as a reduction in material consumption. However, welding often remains the critical factor that governs the overall reliability of such structures.

1.2 Research Motivation

A key challenge when welding HSS is to understand how the process can affect the microstructure and mechanical performance. In addition, HSS are particularly susceptible to hydrogen-induced cold cracking (HICC), especially in the root area, where an increase in hardness makes it easier for the crack to spread.

Traditionally, the standard approach for welding HSS is to at least match the strength of the parent plate (2). In practice, the heat-affected zone (HAZ) and the WM toughness are often lower than those of the BM. To overcome this, the overmatching philosophy tries to ensure that the weld is not considered the weak link, since the weld is the most likely region for stress concentration, caused by fabrication defects, discontinuities, and geometrical effects.

However, for steel grades equal to or greater than S460, an undermatch can be applied (2). The mismatch refers to the difference in strength between the Weld Metal (WM) and the Base Metal (BM). This can be expressed as $M = \frac{\sigma_{WM}}{\sigma_{BM}}$, where σ_{WM} is the strength of the WM and σ_{BM} is the strength of the BM. If $M > 1$, it is called overmatching, and if $M < 1$, it is called undermatching. Finally, if $M = 1$, it is considered matching.

To overcome challenges with welding HSS, the Soft Root Technique (SRT) has been proposed as an alternative concept. The main idea is to introduce an undermatched consumable in the root region, reducing hardness and consequently lowering the likelihood of HICC, while maintaining the overall strength and integrity of the joint. Despite its potential, the application of SRT in HSS remains unexplored in the literature, which motivates the present study.

1.3 Aim and Objectives

The aim of this project is to propose, apply and evaluate an alternative welding technique for HSS, known as SRT.

The specific objectives of this study are:

- To compare the mechanical performance of welded joints produced with matching and undermatched root consumables in S690QL plates of different thicknesses.
- To evaluate the hardness distribution across the weld zone, with particular focus on the root and cap regions.
- To characterise the microstructure of the root-pass area and assess the influence of undermatched consumables on phase formation.
- To analyse dilution effects in the root by means of SEM/EDS and relate them to local mechanical behaviour.

Thus, this research focuses on a clear gap by assessing the feasibility of SRT in S690 thick plates, an area that appears not to be covered in the current literature. In this context, it seeks to support the academic community by sharing insights into best practices for welding HSS. It also offers a critical analysis of existing technical standards in the context of SRT, thereby addressing both the scientific and practical aspects of welding HSS.

Chapter 2

Literature review

This thesis will mainly deal with quenched and tempered HSS. These are known for their strength, excellent weldability, formability, and toughness, making them suitable for use in a variety of heavy duty applications.

This chapter aims to provide an overview of key concepts and previous research relevant to the welding of HSS. A thorough investigation of metallurgical and weldability issues as well as previously solved ones is paramount to support the experiment and analysis performed in the following chapters.

2.1 Low Carbon Steels

The carbon content in steel significantly affects its weldability. Higher carbon increases the risk of forming martensite, a hard and brittle phase, which can cause cracks in the HAZ. Gorni (3) states that steels with a low carbon content ($\leq 0.15\%$) have good weldability, while high-carbon steels ($> 0.30\%$) are more prone to cracking.

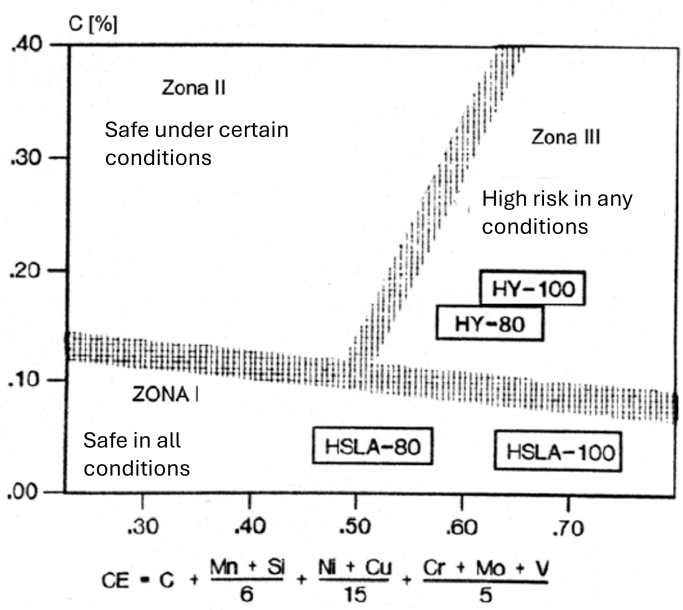

Figure 2.1: Cracking likelihood in the HAZ.

Source: (3) adapted by the author

Generally, the likelihood of cracking in the HAZ depends on the carbon equivalent (CE) and on the welding conditions. As stated in Fig. 2.1, CE is often used to estimate weld-

ability considering other alloying elements. High CE values indicate poorer weldability. To mitigate issues, techniques such as preheating, post-weld heat treatment (PWHT), and low-hydrogen welding can be employed to reduce the risk of cracking and improve joint quality.

However, the hardening mechanisms involved in tempered/quenched or normalised steels depend on their carbon content. Therefore, this is a trade-off between achieving sufficient mechanical strength and ensuring easy machinability and weldability.

To achieve its main purpose, the alloy design should take into account its requirements such as mechanical properties, machinability, durability, cost, and performance in its final application as described by Krauss (4).

2.2 HSS classification

There are various subtypes of HSS, based on their chemical composition, fabrication process, and mechanical properties. These include Dual-Phase (DP) steels, which combine ferrite and martensite, aiming for strength and ductility; Transformation Induced Plasticity (TRIP) steels, known for excellent energy absorption and formability; Complex-Phase (CP) steels, providing high strength with good elongation; and martensitic steels, which are extremely strong but less ductile. Among these, quenched and tempered steels (QT), such as S690QL, emerge due to their exceptional strength and toughness due to heat treatment processes. S690QL, with a minimum yield strength of 690 MPa, is ideal for construction, heavy machinery, and pressure vessels.

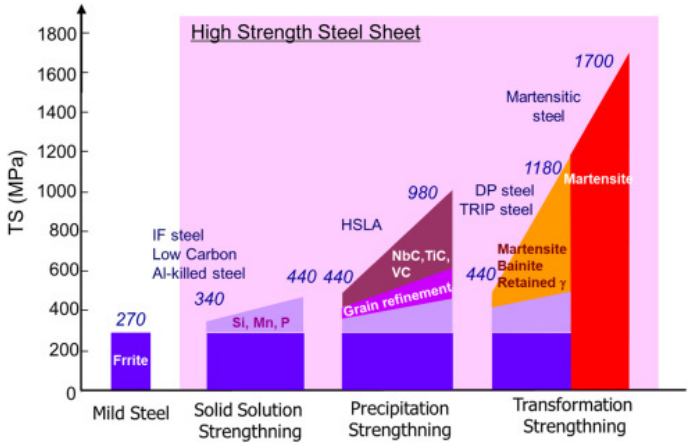

Figure 2.2: Strengthening methods for high strength steel

Source: (5)

2.3 HSS: S690QL

2.3.1 Definition

The term HSS was used for steels with a yield strength between 250 and 700 MPa (Figure 2.3). However, it was increased to 450 to 700 MPa, with S690QL being a common steel among this family (6).

European Standard (7) defines steel as the material of which the majority of elements is iron and contain less than 2% carbon. Furthermore, steels are classified as: non-alloy steels, stainless steels, and alloy steels. HSS are usually classified as alloy special steels, where a specific control of chemical composition is required, and strict controls are imposed on the manufacturing of it.

Beyond this, BS EN 10025-6 (8) defines requirements for the delivery of HSS plates. In accordance with that, S690QL receives its name as:

- **S**: Structural steel;
- **690**: The minimum specified yield strength;
- **Q**: Quenched and tempered;
- **L/L1**: Specified minimum impact energy at $-40\,°C/-60\,°C$.

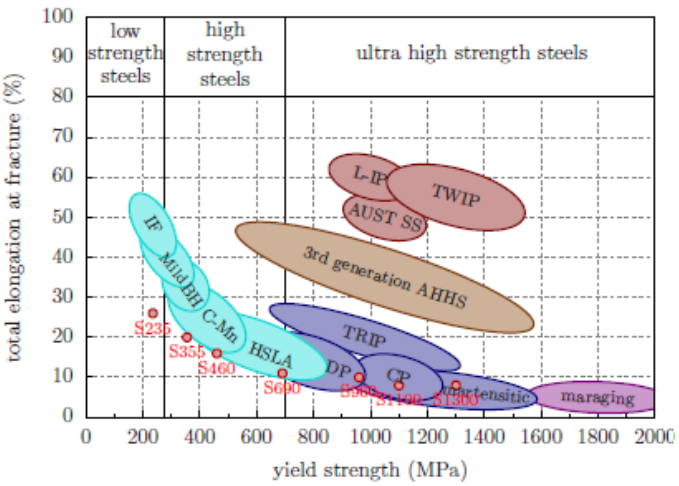

Figure 2.3: Strength and elongation for various steel grades ('banana plot')

Source: (6)

2.3.2 Applications

Koichi (9) brought to the attention the requirements that must be analysed when selecting a material for a defined purpose. According to him, the following are important: (1)

strength-to-weight ratio, (2) fracture toughness, (3) fatigue strength, (4) resistance against corrosion and stress corrosion, and (5) general fabrication requirements (machinability, availability, and cost).

Another important parameter, defined by Alabi et al. (10), is the yield-to-tensile ratio (Y / T).The Y/T ratio provides information on the behaviour of a material under load. A higher Y/T ratio indicates that the material is more brittle, with little plastic deformation before failure. A lower Y/T ratio suggests greater ductility, allowing the material to undergo more deformation before breaking.

For HSS, Eurocode 3 (11) defines a maximum Y/T value of 0.95. However, the UK National Annex to Eurocode 3 (12) recommends a lower maximum value of 0.91. For comparison, mild steels used in the offshore industry typically have a Y / T ratio not greater than 0.85. There is particular concern that increasing the yield strength may reduce ductility, which is crucial for structures subjected to cyclic loads, such as offshore platforms.

The combination of high strength, toughness, and corrosion resistance of S690 steel makes it essential in demanding applications. It is used in stronger bridge structures and high-rise buildings, as well as offshore platforms and wind turbines, because of its resilience in harsh environments. Its toughness under extreme stress also suits it for mining, construction machinery, and pressure vessels (13).

2.3.3 Metallurgical considerations

Many structural steels are produced using TMCP. However, for HSS, there are restrictions when producing thicker sections (14). Therefore, quenching and tempering became the preferred processing route, as shown in Figure 2.4, where the influence of process selection and CE is illustrated for a specific thickness range.

In order to combine strength, toughness, and weldability, metallurgists have been working to find the best formula. The following general principles are applied to S690 and other HSS to achieve the requirements.

- Lower carbon content helps improving weldability and toughness;
- Finer grain sizes (ferrite or bainite) micro alloying usually with Nb, V and Al , providing increased strength and toughness;
- Greater quality control to reduce impurities such as S, P, and O;
- Alloying elements such as Ni, Cr, Mo and Cu to provide solid solution and transformation strengthening.

2.3.4 Weldability

One common way to assess the weldability of steels is to analyse their toughness and their tendency to Hydrogen-Induced Cold Cracking (HICC) in the HAZ. In the case of S690, a

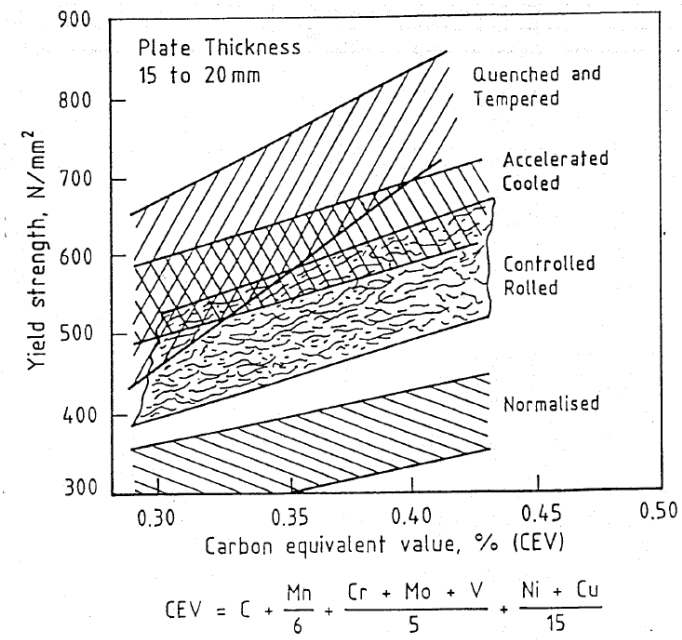

Figure 2.4: Processing routes for steels

Source: (14)

high-strength quenched and tempered steel, both aspects become particularly critical due to their elevated yield strength and increased hardenability (15).

The strength of S690 is a combination of alloying elements. Carbon, manganese, and niobium improve strength and promote hardenability. However, while nickel increases the fracture toughness, copper helps with corrosion.

However, there is a trade-off as the alloying content increases along with the risk of forming brittle microstructures. Therefore, cold cracking becomes more likely, especially in the HAZ and sometimes in the WM itself.

In order to match the strength of the BM, filler metals also require a higher alloy content, which comes with a cost. The increased alloying in consumables raises diffusible hydrogen levels and also tends to reduce the toughness of the WM. Combine that with high residual stresses from welding, the risk of HICC increases, particularly in thick sections or highly restricted joints Figure 2.5.

Controlling this risk is possible through the implementation of quality controls such as adequate preheating, limiting heat input, using low-hydrogen consumables, and designing joints to reduce restraint. Applying these strategies correctly will manage cooling rates and mitigate cracking initiation.

As shown in Tab. 2.1, each alloying element plays a different role which explains the microstructure and mechanical properties. Molybdenum and boron, for instance, promote bainite or martensite formation, increasing hardenability, and also increasing susceptibility to cold cracking. Grain refiners and strong ferrite strengtheners such as Nb, V, and Ti enhance mechanical performance while providing precise control during welding to avoid

the formation of coarse and brittle structures. (15)

In summary, while alloying gives S690 its strength and versatility, it also introduces challenges to weldability. A clear understanding of how these elements interact with the thermal cycles during welding is key. This allows for better control, fewer defects, and greater confidence in the whole process.

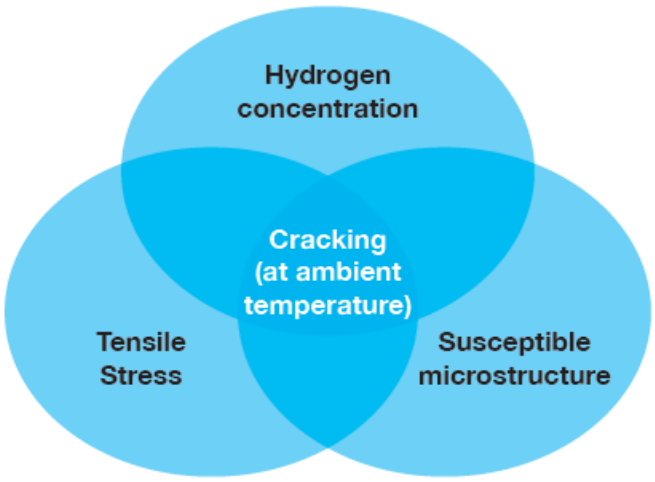

Figure 2.5: Necessary factors to cause hydrogen cracking

Source: (15)

2.4 Mismatching and the soft root technique

In general, the microstructure of a steel controls its strength. Therefore, the chemical composition, thermal history, and deformation process during production play an important role in indirectly controlling the strength. Taking into account the different applications mentioned above, S690 must be available in a significant range of thicknesses (30mm-100mm), as well as exhibit good weldability and toughness (14).

There are several possible techniques that can be employed to reach the desired requirements while welding. One of them is to use welding consumables to match, overmatch, or undermatch. SRT uses a lower consumable in the root to reduce the hardness of the welding zone.

Umekuni and Masubuchi (16) applied this technique to the root of HSS such as HY-100 and HY-130, commonly used for military purposes. In their study, the first welding pass was performed using an undermatching consumable. The primary objective of the research was to understand crack propagation behaviour while reducing preheating requirements. The results showed that both matching and undermatching samples exhibited the same crack propagation rate. However, samples where the SRT was applied required significantly less preheating, which could improve productivity without compromising safety.

Rak et al. (17) investigated the use of SRT in welded joints using HT80 steel. Even with

Table 2.1: Alloying elements frequently used and their roles

Element	Role
C	Strengthener
Mn	Delays austenite decomposition during accelerated cooling
	Decreases ductile to brittle transition temperature
	Strong sulphide former
Si	Solid solution strengthener
	Deoxidiser in molten steel
Al	Deoxidiser
	Limits grain growth as AlN
Nb	Very strong ferrite strengthener as Nb(C,N)
	Delays y–alfa transformation
Ti	Austenite grain size control by TiN
	Strong ferrite strengthener
V	Strong ferrite strengthener by V(C,N)
Zr	Austenite grain size control by Zr(C,N)
	Strong sulphide former
N	Forms nitrides and carbonitrides with Ti, V and Al
Mo	Promotes bainite formation
	Ferrite strengthener
Ni	Increases fracture toughness
Cu	Improves corrosion resistance
	Ferrite strengthener
Cr	With Cu increases atmospheric corrosion resistance
B	Promotes bainite formation

mismatch ratios as low as 0.57 in the root, and considering 25-45% of the undermatched WM, they found that fracture toughness remained acceptable and crack redirection could occur toward the BM. These results support the idea that softer root does not necessarily degrade mechanical performance.

Mochizuki and Kawabata (18) studied the use of HT950 for penstocks in a hydropower plant in Japan. They conducted both numerical and experimental analyses to compare the overmatching and undermatching welding processes in the steel under investigation. The motivation for this research arose from the challenges encountered in the welding of HSS. As stated in the study, one possible solution could be the development of steel that does not require preheating. However, this would not only increase costs, but also complicate non-destructive testing (NDT) because of the high levels of austenite present. In the end, they demonstrated that both samples exhibited the same levels of tensile strength.

Building on these findings, Loureiro (19) conducted a study on the tensile properties of undermatched welds in quenched and tempered HSS, RQT701 (British Steel). Two different heat inputs were applied to achieve different mechanical properties in both the WM and the HAZ. The research focused on analysing the microstructure and mechanical properties of the welded joints. The higher heat input coarsened the microstructure and reduced the hardness in the WM and HAZ. The increased heat input led to a reduction

in both yield and tensile strength in the WM and HAZ, amplifying the undermatching condition between the WM and the BM.

More studies were produced in this field, especially to seek solutions for welding steels with yield stress higher than 700 MPa, which create challenges to produce WMs with yield stress higher than that and making it unfeasible to apply an overmatch technique (20).

Although these works provide important observations into the use of undermatched consumables and the SRT concept, most were carried out on steels such as HY-100, HT80, HT950 or RQT701, often in military or specialised applications. They do not address modern quenched and tempered steels like S690, widely used in civil and offshore structures, nor do they systematically investigate thick sections where welding challenges are more severe. This points out a clear knowledge gap, demonstrating the relevance of investigating SRT in another group of steels that are commonly used.

2.5 Investigations in HSS Welding

When proposing a different technique in any field of science, it is important to look for benchmarks that can be used to evaluate the performance of the work being carried out. Different industries have performed experimental studies to analyse microstructural transformations, mechanical performance, and critical issues such as cracking or hardness variations. These will be presented in this chapter and compared with the results shown in Chapter 4.

2.5.1 Laser Welding of HSS

Laser Beam Welding (LBW) is well known for its productivity and is widely used in the automotive industry. However, the naval sector has also been trying to implement these techniques in shipyards. A recent study explored the laser-arc hybrid welding process applied to EH36 plates, commonly used in ship construction. In order to understand the influence of groove width on weld quality (21), several experiments were conducted which indicated that narrower grooves led to arc deflection and interruptions, along with increased martensitic formation due to rapid cooling. In contrast, wider grooves promoted bainite formation and reduced hardness gradients. Mechanical testing showed that the welds achieved high levels of tensile strength (553 MPa). The study brought attention to another parameter when developing welding procedures, namely the groove design, especially in thick sections.

LBW was also investigated as a single-pass high-speed possibility for 15mm S690 steel, as cost and time are challenges when welding thicker sections. However, experimental tests using these plates under restricted conditions revealed a correlation between solidification cracking and the intensity of the restraints (22). The experiments performed showed that critical stresses were induced during the solidification of the melt pool in such a way that the use of LBW in HSS requires mitigation strategies to ensure the reliability of the structures, although it offers high productivity.

2.5.2 Hardness and Microstructure in S690QL Welded Joints

In the context of offshore structural applications, Mendes et al. examined the microstructure and hardness profiles of S690QL welded joints (13). The main goal was to understand how the final welding passes affect the previous ones. They tested 2 different thicknesses: 30mm and 60mm, both fully and partially welded. With that, they could understand the difference in hardness that was caused in the root through a Vickers hardness survey. The results provided reinforce the importance of PWHT and the implementation of strict quality controls during welding activities in order to minimise residual stress and prevent brittle phases, particularly in structures where cyclic loading is an important design variable.

2.6 Challenges and Research Gaps

A quantitative and qualitative literature review was conducted using the Bibliometrix tool (23). The following search strategy was applied to both the Scopus and Web of Science databases to identify relevant publications for this research:

- **(TITLE-ABS-KEY (”hss” OR ”high yield”) AND TITLE-ABS-KEY (”steel”) AND TITLE-ABS-KEY (”undermatch” OR ”soft”) AND TITLE-ABS-KEY (”welding”))**

As expected, only a limited number of publications were found (Tab. 2.2), highlighting a research gap in the field of welding, particularly in terms of undermatched or SRT in HSS. The data presented in Tab. 2.2 reflect combined results from both Scopus and Web of Science.

It should also be noted that the only two articles specifically addressing the SRT and discussed in 2.4 are not indexed in either of these databases, suggesting that studies on this subject may be scarce or remain unpublished in widely accessible academic platforms.

Table 2.2: Analytical Literature Review

Document type	Number of documents
Article	5
Conference Review	3
Conference Paper	2
Book Chapter	1
Total	**11**

2.7 Summary

Chapter 2 presented an overview of the welding of HSS. Important characteristics such as mechanical properties and weldability were explored through studies focusing on different industry sectors, including offshore and civil construction.

The **SRT** can be an effective strategy to reduce excessive hardness in the root of the weld and, therefore, its susceptibility to HICC, without compromising overall strength. However, most of these studies were carried out on steels intended for military applications. They did not address quenched and tempered steels such as S690, which are widely used in civil engineering, offshore, and energy sectors.

This persistent gap highlights the need for further investigation, which frames the relevance of the present study.

Chapter 3

Methodology

This chapter details the materials, equipment, and procedures used during experimental work. The SRT will be detailed along with the test methods applied to evaluate mechanical and metallurgical performance.

3.1 Materials

Given the applications presented in Section 2.3.2, the material selected as the BM was S690QL1, delivered according to BS EN 10025-6 (8). Two plates were welded with thicknesses of 50 mm and 35 mm. The chemical composition and mechanical properties of the material are given below.

Element	**S690 (50 mm)**	**S690 (35 mm)**	**Requirement (8)-max**
C	0.162	0.196	0.22
Si	0.292	0.474	0.86
Mn	1.29	1.533	1.80
P	0.013	0.014	0.025
S	0.0006	0.0007	0.012
N	0.0042	0.0037	0.016
Cu	0.022	0.032	0.55
Mo	0.22	0.012	0.74
Ni	0.12	0.03	4.10
Cr	0.321	0.043	1.60
V	0.001	0.001	0.07
Nb	0.024	0.023	–
Ti	0.005	0.015	0.07
B	0.0017	0.0014	0.006
Zr	0.00002	0.0002	0.17
Al+T	0.07	0.036	–
C_{eq}	0.49	0.47	0.65

Table 3.1: Chemical composition of the base materials and standard limits according to EN 10025-6 (values in wt.%)

Mechanical Property	**S690 (50 mm)**	**S690 (35 mm)**	**Requirement (8)**
R_{eH} [MPa]	807	781	≥ 690
R_m [MPa]	854	856	770–940
Impact energy ($-60\,^{\circ}$C [J])	140	104	≥ 27

Table 3.2: Mechanical properties of the S690QL1 plates and requirements

3.2 Consumables

The main concept of this research was to use two different consumables as a weld metal and to analyse the role each of them would play. The undermatching consumable used was a Fluxed Cored Wire (FCW) (classified according to EN ISO 17632-A: T 46 4 M M 1 H5), which has lower mechanical strength and improved ductility compared to the parent metal. The matching consumable used was a FCW (classified according to EN ISO 18276-A: T 69 6 M M 1 H3), which provides mechanical properties similar to those of the S690QL1 parent metal.

These specific consumables were selected according to the qualified procedures of the industrial partner, which ensures realistic applicability. At the same time, they allow for a direct comparison between matching and undermatching strategies, which is a central topic in this research. Classification, properties, chemical compositions and explanation for designation codes are described in Tab. 3.3, Tab. 3.4 and Tab. 3.5.

Property	**Tubrod 15.17**	**WB 6132**
Standard	EN ISO 17632-A	EN ISO 18276-A
Classification	T 46 4 M M 1 H5	T 69 6 M M 1 H3
Type	FCW	FCW
Yield Strength (MPa)	$\geq$460	$\geq$690
Tensile Strength (MPa)	500–640 (typical)	760–900 (typical)
Impact Toughness	$\geq$47 J at –40 °C	$\geq$27 J at –60 °C
Hydrogen Diffusible	$\leq$5 ml/100g (H5)	$\leq$3 ml/100g (H3)

Table 3.3: Classification and properties of welding consumables

Element	EN ISO 17632-A: T 46	EN ISO 18276-A: T 69
C	0.05	0.075
Si	0.34	0.45
Mn	1.15	1.75
Cu	-	0.15
Mo	-	0.55
Ni	0.96	2.25
Cr	-	0.45
C_{eq}	0.31	0.73

Table 3.4: Chemical composition (wt.%) of filler wires used in the welding procedures.

Code	Meaning
T	Tubular (flux-cored) wire
46 / 69	Minimum tensile strength: 460 MPa / 690 MPa
4 / 6	Minimum impact energy at temperatures: –40 °C (4) and –60 °C (6)
M	Shielding gas: M21 (Ar+CO_2)
M	Welding position: all positions
1	Polarity: DC+, electrode positive
H5 / H3	Hydrogen level $\leq$5 ml (H5)/ $\leq$3 ml (H3) per 100 g of weld metal

Table 3.5: Explanation of the designation codes for tubular welding consumables according to ISO standards

3.3 Welding Process and Equipment

FCAW (flux cored arc welding) was the fusion welding process used in the experiment. Combining an external shielding gas with an internal flux, FCAW-G employs tubular wires, providing extra protection for the weld pool, increasing the stability of the arc and reducing the amount of spatter.

This welding process is widely used in industry to weld thick plates because it offers high deposition rates and a stable spray transfer. Providing a higher heat input compared to other fusion welding techniques, it slows down the cooling rate, which mitigates the risk of HICC.

The power source used during the procedure was a TERRA NX 400 PMC in combination with the WF 300 wire feeder.

3.4 Welding Procedure and experimental set up

Using a proven WPQR, already qualified by the industry partner, which guarantees the applicability of the results, two plates were welded as shown in Figure 3.3. The dimensions of the plates were 400 mm × 200 mm, with two different thicknesses: 35 mm and 50 mm, as described in Section 3.1. On each of the plates, two different welding runs were performed. Half of each plate was fully welded using a matching consumable, and the other half was welded using a combination of undermatching and matching consumables (Figure 3.4). The characteristics of the consumables are described in Table 3.3 and Table 3.4.

The plates were prepared with a single V bevel and a ceramic backing, the latter being the standard practice of the industrial partner, as shown in Figure 3.1 and Figure 3.2. In both plates, when applying the SRT (Figure 3.5), a 12 mm height section of the plate was welded with a lower strength consumable, a value chosen as a reasonable proportion for sensitivity analysis. This corresponds to 34% of the 35mm plate and 24% of the 50mm plate made with a consumable of lower strength. Therefore, the aim is to analyse two different variables: the use or non-use of the SRT, and the impact of increasing the

amount of undermatching consumable over the plate thickness.

Furthermore, the welding parameters applied in the experiment are described in Table 3.6. It is important to note that the weld mark references defined in Table 3.7 will be used throughout this report.

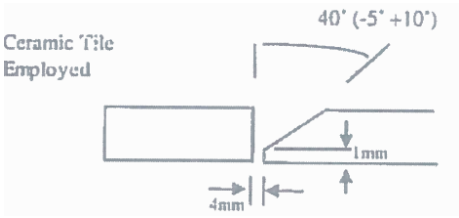

Figure 3.1: Bevel geometry used

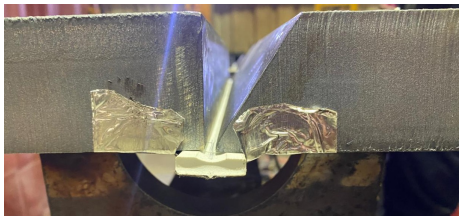

Figure 3.2: Bevel type with ceramic backing

Figure 3.3: Welding procedure

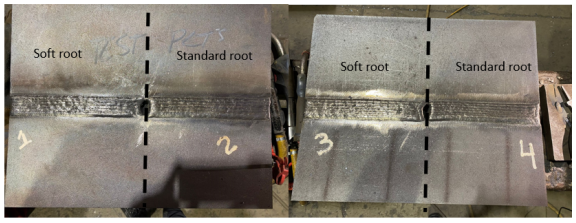

Figure 3.4: Welded plates and their marks

Figure 3.5: Soft root vs Standard method schematic

Pass	**Position**	**Wire (mm)**	**Voltage (V)**	**Current (A)**	**Weld Speed (mm/min)**	**Heat Input (kJ/mm)**
Root run	PA	1.2	19–20.5	174–182	74–80	1.98–2.42
Hot pass	PA	1.2	20–21.5	209–222	112–120	1.67–2.04
Fill	PA	1.2	20–23	188–226	105–220	0.82–2.37
Cap	PA	1.2	19–21	177–194	164–190	0.85–1.19
Polarity: DCEP		Gas Flow: 15–20 L/min		Shielding Gas: 80% Ar, 20% CO_2		
Preheat: 150°C		Heating Method: Propane torch		Max Interpass Temp: 250°C		

Table 3.6: Welding parameters used in the experiment.

Mark run	Thickness	Welding technique	Material	SRT (%)
1	35 mm	Soft Root	S690	34
2	35 mm	Standard	S690	0
3	50 mm	Soft Root	S690	24
4	50 mm	Standard	S690	0

Table 3.7: Weld identification by mark number and corresponding SRT proportion.

3.5 Laboratory Testing and Characterisation Methods

This section outlines the test plan and characterisation methods used. Given the high strength of the BM, some procedures required industrial facilities.

3.5.1 Macroscopic and Microscopic Examinations

In accordance with BS EN ISO 17639 (24), plates were cut as depicted in Figure 3.6 to produce one macro sample per welding run.

In addition, Figure 3.7 presents the cutting plan for the microanalysis. An additional sample from the BM was extracted to provide a baseline for comparison with the HAZ and the WM.

Using University facilities, a series of preparation processes, including etching, grinding, and polishing, were carried out. Details are described in Table 3.8.

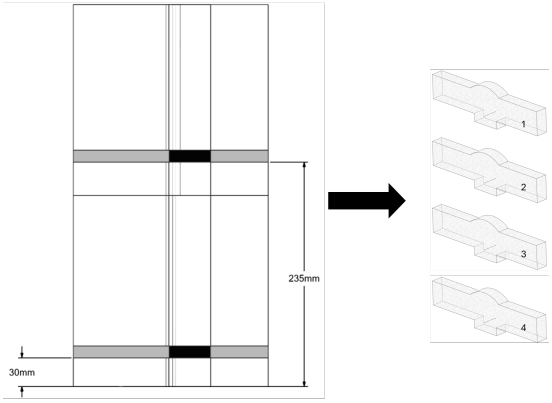

Figure 3.6: Cutting plan for Macroscopic examination

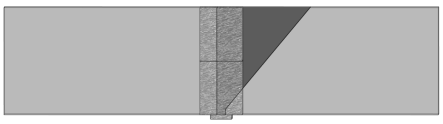

Figure 3.7: Schematic of Microscopic Samples (hatched area)

Grinding	Sandpaper used: 240/1200/2500 grit	Until scratch marks minimised
Pre-polish	3 µm water-based diamond	4 min 30 s
Polish	0.04 µm colloidal silica	2 min
Etching	2% nital	8 s

Table 3.8: Specimen preparation for microanalysis

3.5.2 Hardness Survey

A hardness survey was conducted as described in Table 3.9 and illustrated in Figure 3.8. Vickers hardness tests were performed with a load of 1 kgf (HV1) at room temperature on the samples shown in Figure 3.6. The tests were performed using a Falcon 503 microhardness tester from Innovatest.

Indentation lines were placed to capture WM, HAZ and BM, allowing the hardness profile across the joint to be evaluated.

Sample	Region	Rows	Row spacing	Indents per row	Row length
1 & 2 (35 mm)	Bottom	3	5 mm	30	30 mm
1 & 2	Cap	3	5 mm	50	50 mm
1 & 2	Vertical	1	—	30	30 mm
3 & 4 (50 mm)	Bottom	3	5 mm	50	50 mm
3 & 4	Cap	3	5 mm	60	60 mm
3 & 4	Vertical	1	—	40	40 mm

Table 3.9: Summary of hardness survey

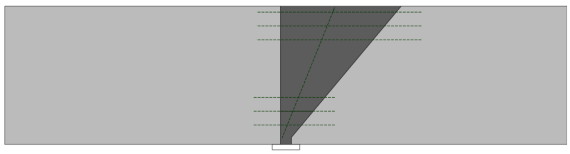

Figure 3.8: Hardness survey lines

3.5.3 SEM

Chemical characterisation was performed using Energy Dispersive Spectroscopy (EDS) coupled with a Scanning Electron Microscope (SEM), with parameters described in Table 3.10. The purpose of this analysis was to characterise inclusions and determine the composition along the weld zone to understand the dilution of the different weld metals used with the SRT. In addition, high-resolution images were obtained at high magnification. The SEM-EDS system provides elemental spectra and compositional data from selected regions of the sample.

Parameter	Value	Meaning / Function
Detector	E–T (Everhart-Thornley)	Used for **secondary electrons (SE)** to provide high-resolution surface imaging.
Beam Current (BC)	1 nA	Electron beam current delivered to the sample.
FOV (Field of View)	56.8 μm	Total area visible in the image.
WD (Working Distance)	6 mm	Distance between the sample surface and the detector.
Speed	6	Scan speed setting of the instrument.
Scan Mode	EDS analysis	Mode selected for elemental composition analysis.
Magnification (Mag)	5 kx	Image magnification (5000× actual size).

Table 3.10: SEM parameters used for analysis

A vertical line, as shown in Figure 3.9, was defined to investigate the compositional variation along the weld zone. The cross section was divided into two regions, labelled as A and B. For each region, 10 points were analysed: at each point, a high-resolution image was captured, and the chemical composition was measured using EDS. In addition, three horizontal lines were also examined in sample 3B (soft root – 50 mm), specifically positioned near the interface between the undermatching and matching WMs, to assess local dilution effects.

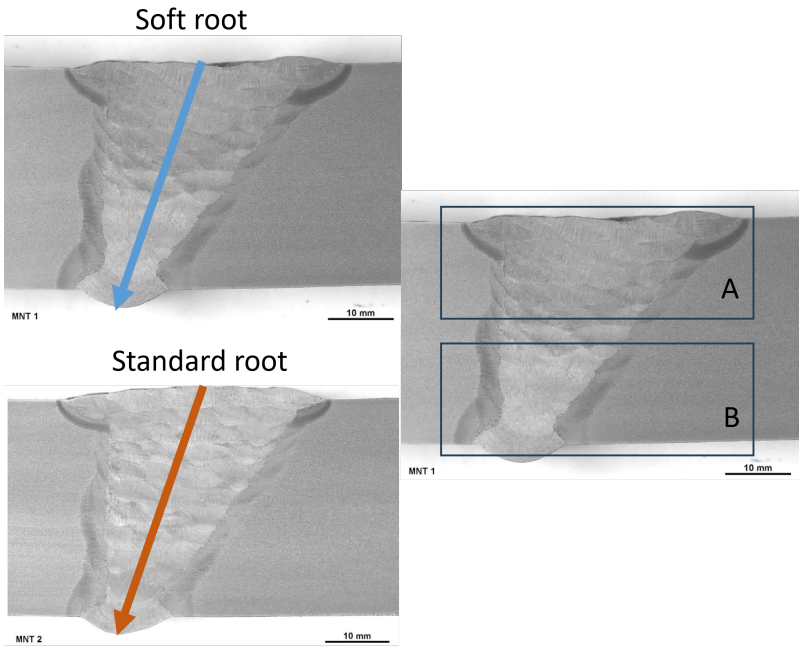

Figure 3.9: SEM analysis strategy

3.5.4 Tensile Testing

According to BS EN ISO 4136 (25), tensile tests were carried out. Due to the maximum dimensions of the tensile specimen, the thicker sections (50 mm) were divided into two samples, as shown in Table 3.11. This not only allowed compliance with testing requirements, but also permitted the mechanical performance of the cap and root regions to be assessed separately, which is relevant for the aims of this research.

Sample No.	**Description**	**Width (L_c) (mm)**	**Thickness (b_0) (mm)**
1	Plate 1 (35 mm)	25.2	33.6
2	Plate 2 (35 mm)	24.9	33.8
3-A	Plate 3 (50 mm) – Cap	24.9	26.8
3-B	Plate 3 (50 mm) – Root	24.9	26.7
4-A	Plate 4 (50 mm) – Cap	24.9	25.2
4-B	Plate 4 (50 mm) – Root	24.9	25.6

Table 3.11: Dimensions of the tensile test specimens.

Figure 3.10 illustrates the cutting plan used for the tensile tests. In addition, Figure 3.11 presents a schematic of the specimen used, with its dimensions detailed in Table 3.11 per sample number.

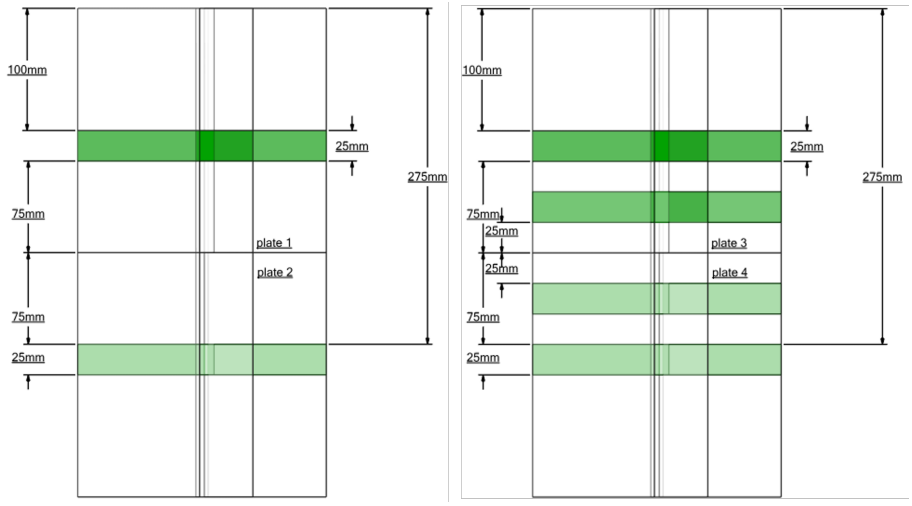

Figure 3.10: Cutting plan for tensile specimens

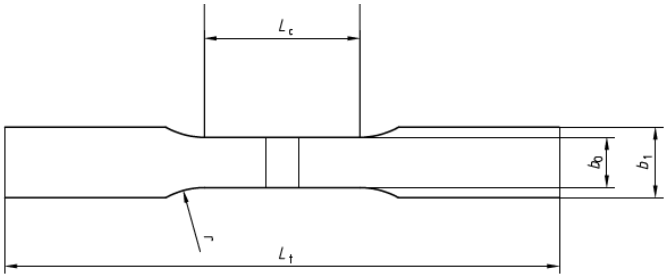

Figure 3.11: Tensile test specimen

3.5.5 Impact Testing

According to BS EN 9016 (26), Charpy impact tests were performed. Figure 3.12 and Figure 3.13 illustrate the cutting plan used for these tests.

Specimens with a V-notch were extracted from the bottom region of both plates to compare the performance of the welded root area. A total of 12 samples were tested, three from each type of weld pass, as described in Table 3.7. The tests were carried out at $-60\,^{\circ}\mathrm{C}$.

The test temperature was chosen to be consistent with the classification of BM, whose toughness is specified at this temperature (Table 3.2). In addition, assessing the root region at such low temperature provides relevant information for structural applications exposed to cold or demanding service conditions, where fracture resistance is critical.

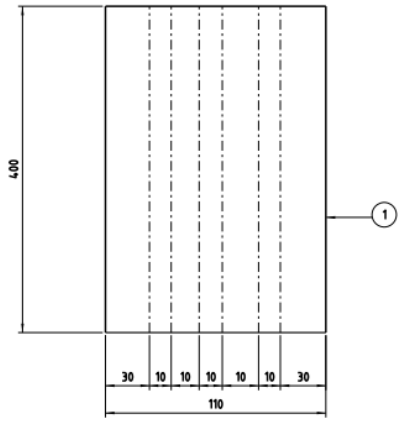

Figure 3.12: Specimens quotation

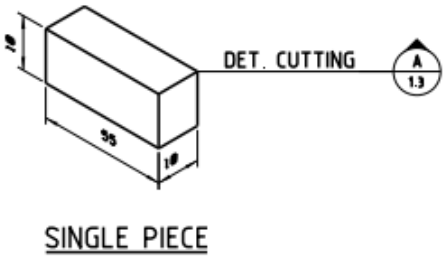

Figure 3.13: Specimens quotation

3.6 Methodological Justification

Given the methods selected in this study, each is expected to provide answers that, together, support the use of the SRT. The welding procedure was based on an industrially qualified procedure, ensuring the applicability of the proposed technique. Furthermore,

the innovation of this research does not lie in the welding procedure itself, but in the use of different consumables, which are expected to yield different results from the standard and already known approach. Finally, the choice to weld thicker plates establishes certain limitations on the experiment, since it demands industrial capabilities for welding, cutting, and specimen preparation. However, it also fills gaps in the literature and provides findings that can be applied in real world practice.

Chapter 4

Results

4.1 Macroscopic Examination

Macrographs of the welded joints for all conditions (Samples 1 to 4) are shown in Figure 4.1. Although sample 2 appears to be without defects, sample 4 exhibits a clear lack of fusion near the root area. The weld beads across all samples exhibit a conical pattern of a multipass welding process, with good fusion between layers. The bead width remains consistent among the samples, indicating a well-controlled procedure. However, small differences are observed in the geometry of the root area. In Samples 1 and 3, which used a filler metal with lower yield strength, the root appears slightly narrower and more rounded (Figure 4.2).

Although macrographic analysis does not provide definitive conclusions about mechanical performance, it offers important visual hints about the welding process and joint quality. These observations are reported for later comparison with the mechanical test results.

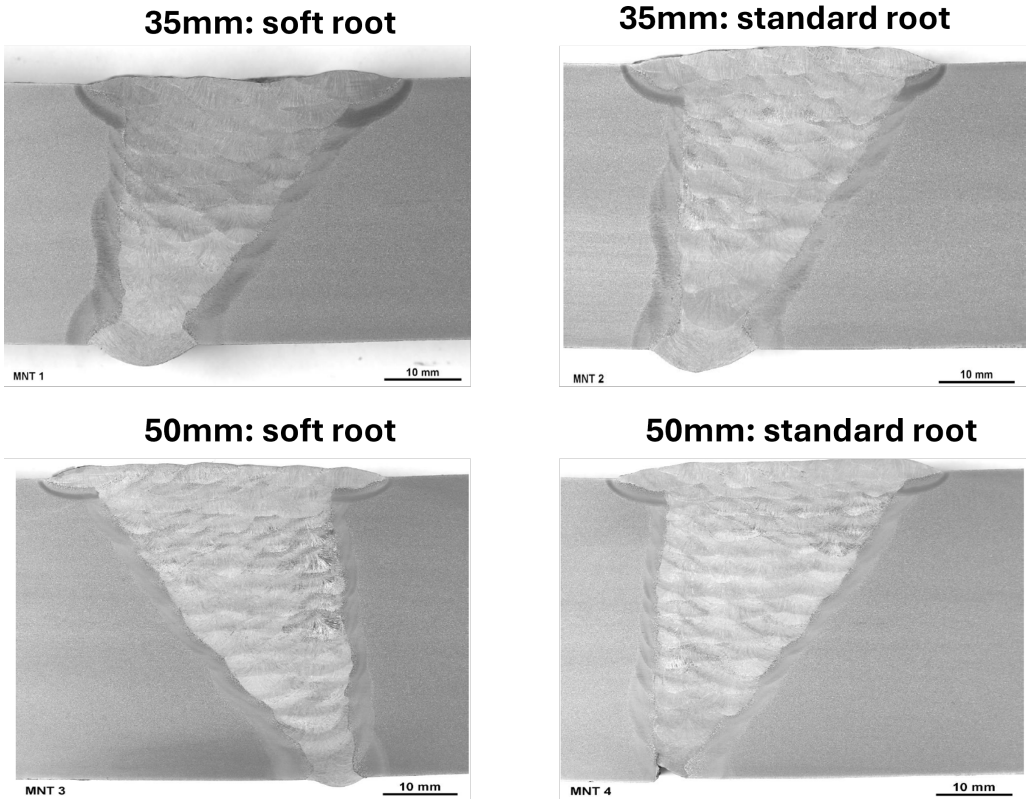

Figure 4.1: Macro samples for Plates 1 to 4

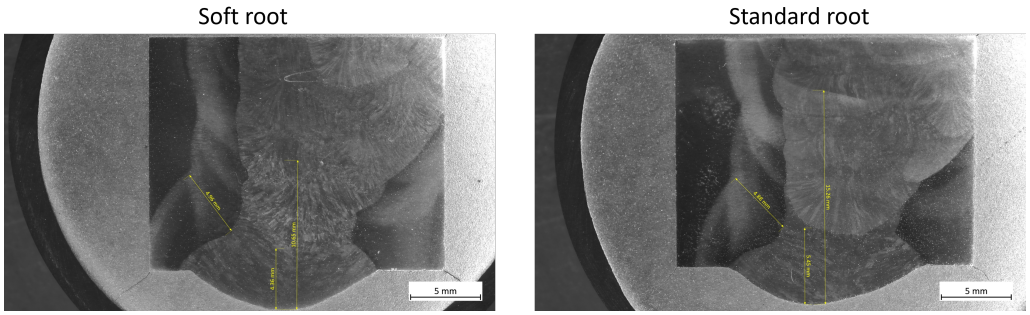

Figure 4.2: Micro samples for Plates 1 and 2

4.2 Microscopic Examination

Figure 4.3 presents the optical microscopy images of the BM (a), the soft root (b), and the standard root (c), the latter two taken from the root area of joints 1 and 2, respectively. At first glance, the micrographs were challenging to analyse. However, further reading of the literature confirms that the microstructure of quenched and tempered high-strength steels (HSSs), typically composed of BCC (body-centred cubic) phases such as martensite and bainite, is inherently difficult to distinguish using standard optical microscopy techniques (27).

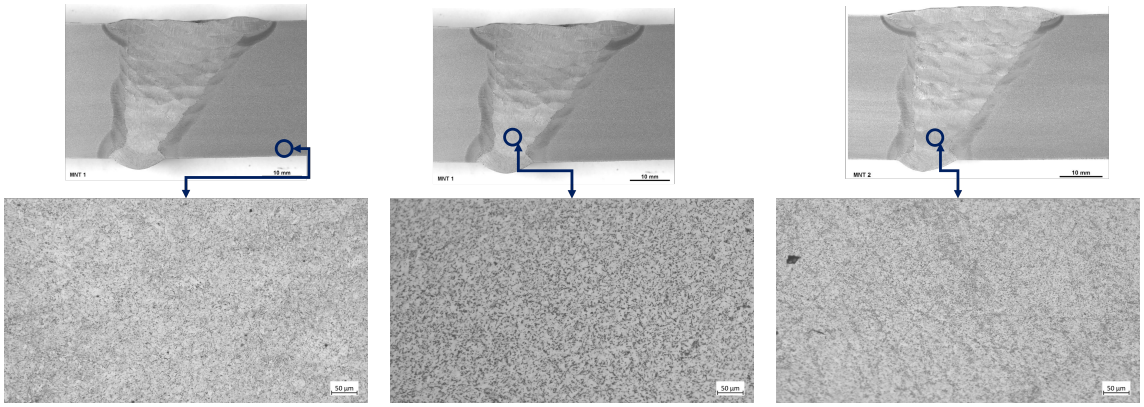

(a) Parent material (b) Soft root (c) Standard root

Figure 4.3: Microstructural analysis by optical microscopy: (a) base metal, (b) soft root weld metal, and (c) standard root weld metal.

The microstructure of the BM, shown in Figure 4.3a, presents a fine and homogeneous morphology, typical of a quenched and tempered steel. Given a carbon equivalent of 0.47 (Table 3.1) and a relatively high manganese content (1.53 wt.%), the microstructure is consistent with tempered martensite and/or bainite, as expected for S690QL steel. No clear evidence of polygonal ferrite was observed, as there are no rounded grains or well-defined boundaries visible, characteristics of this phase. Furthermore, this microstructure aligns with the description in Table 2.1, which highlights the role of manganese in promoting the formation of martensite and bainite by delaying the decomposition of austenite.

Figure 4.3b corresponds to the soft root region, welded using Tubrod 15.17 (Table 3.3). Considering its alloying composition and low carbon equivalent ($C_{eq} = 0.31$), the formation of softer microstructures is expected, depending on the cooling rate. However, because of the limitations of optical microscopy, phase boundaries are not clearly resolved, which makes it difficult to distinguish bainite from ferrite. Therefore, SEM imaging, together with hardness testing, is likely to provide a more accurate characterisation of the microstructure in this region.

Figure 4.3c shows the microstructure of the standard root, welded using WB 6132. Significantly different from Tubrod 15.17, this consumable has a much higher carbon equivalent ($C_{eq} = 0.73$) and is characterised by a higher alloying content, including Ni, Mo, and Mn. The micrograph appears slightly more heterogeneous and possibly coarser. However, because of the inherent limitations of optical microscopy, detailed interpretation remains inconclusive.

To overcome the limitations of optical microscopy and confirm the presence of specific microconstituents, SEM was subsequently performed and presented in Section 4.4.

4.3 Hardness profile

As described in Section 3.5.2, a hardness mapping was performed on the welded joints, comparing the two techniques. Measurements were taken at different positions as described in Table 3.9. Figure 4.4 to Figure 4.13 illustrate the hardness variations observed.

Furthermore, Figure 4.14 to Figure 4.16 present box plots of the hardness profiles, which not only allow for comparison of mean hardness, but also highlight the standard deviation and the overall spread of the measurements for each measured line.

As depicted in the graphs, the horizontal hardness profile for the bottom section of the weld (near the root area), comparing the soft root and standard root conditions, exhibits significantly lower hardness values in the root region compared to the standard root. This confirms that the SRT successfully reduces the hardness at the weld root, which was a primary objective of the method. However, in the top region of the weld, as the same WM and the same weld parameters were applied, the differences become less pronounced as expected.

From Table 4.1, a general assessment of the impact of the method is presented. For the thinner plate section (35 mm), a 13.2% reduction in the vertical line is observed. For horizontal lines near the root, the reduction reaches approximately 10%. In the thicker plate (50 mm), the reductions are less evident, with a 7.3% decrease in the vertical line and around 5% in the horizontal lines. This difference is consistent with expectations, as the proportion of filler material of lower strength used in the joints varied, as described in Table 3.7.

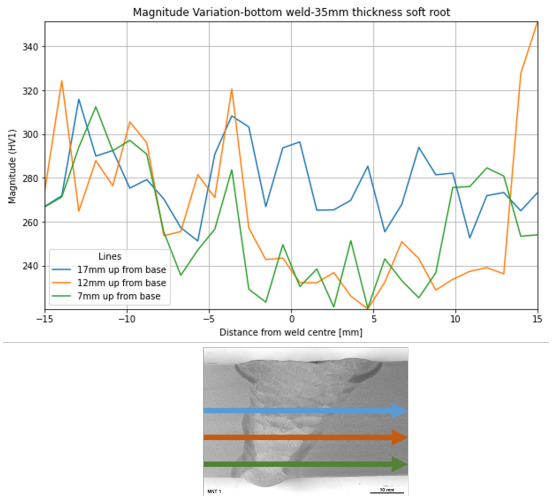

Figure 4.4: Hardness for Plate 1: bottom

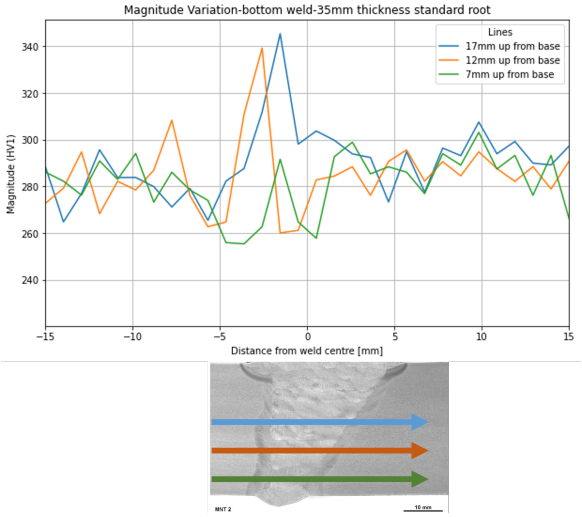

Figure 4.5: Hardness for Plate 2: bottom

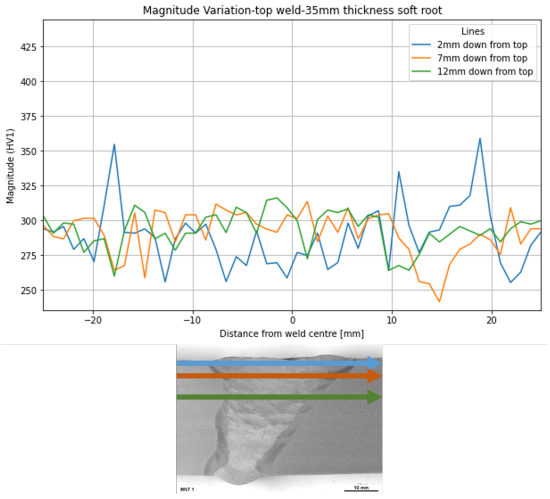

Figure 4.6: Hardness for Plate 1: cap

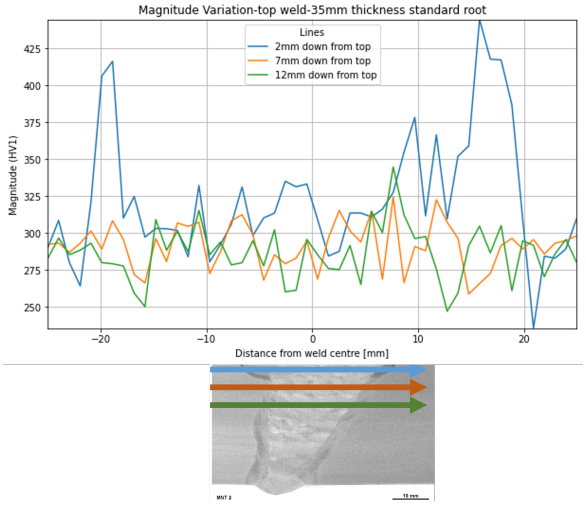

Figure 4.7: Hardness for Plate 2: cap

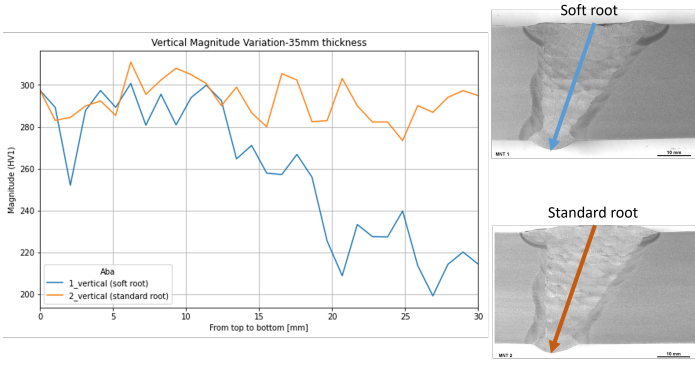

Figure 4.8: Hardness for Plate 1 and 2: vertical line

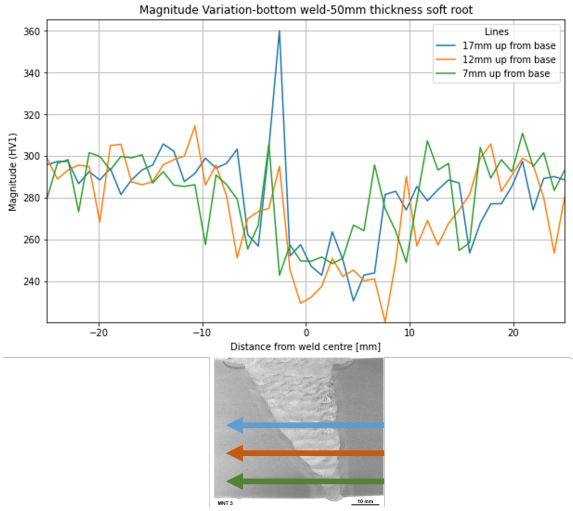

Figure 4.9: Hardness for Plate 3: bottom

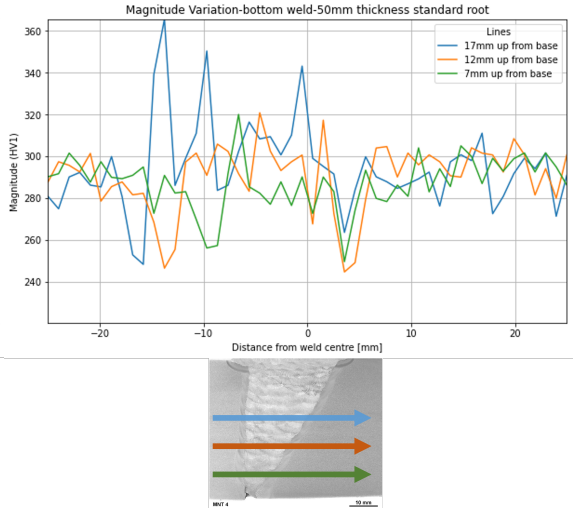

Figure 4.10: Hardness for Plate 4: bottom

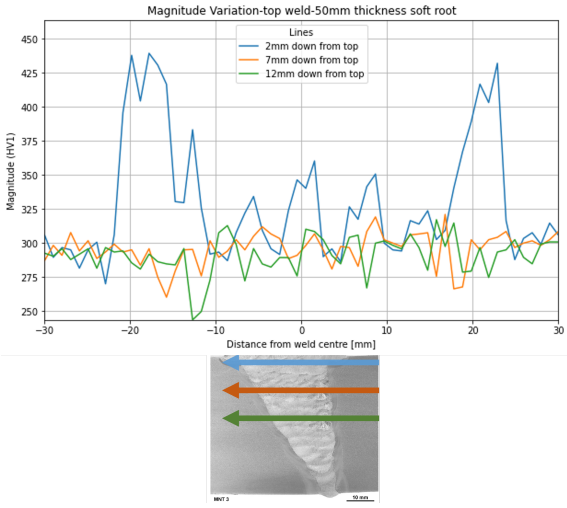

Figure 4.11: Hardness for Plate 3: cap

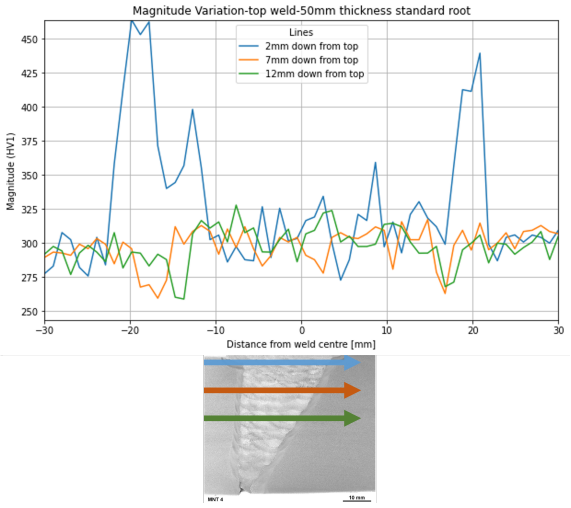

Figure 4.12: Hardness for Plate 4: cap

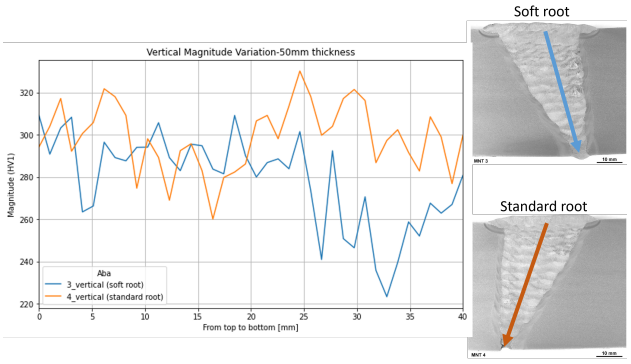

Figure 4.13: Hardness for Plate 3 and 4: vertical line

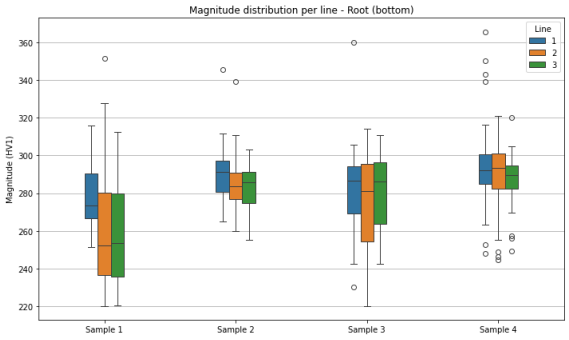

Figure 4.14: Box plot for root region

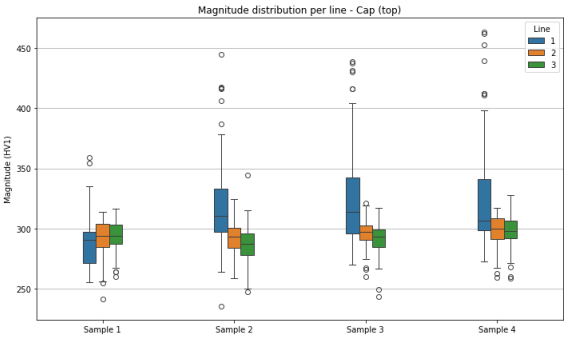

Figure 4.15: Box plot for cap region

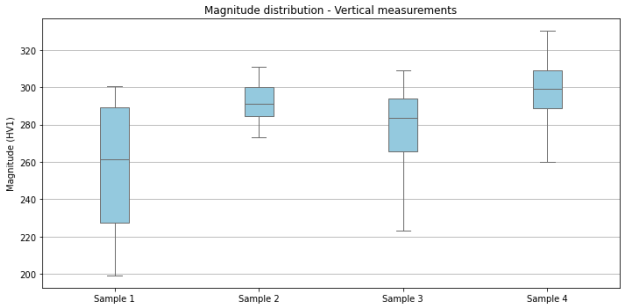

Figure 4.16: Box plot for vertical survey

Position	**Line**	Δ Mean (S1 – S2) [%]	Δ Mean (S3 – S4) [%]
Bottom	1	-12.8 (-4.6%)	-13.7 (-4.9%)
Bottom	2	-22.0 (-8.4%)	-15.1 (-5.5%)
Bottom	3	-23.7 (-9.2%)	-6.5 (-2.3%)
Top	1	-34.4 (-11.9%)	+3.1 (+0.9%)
Top	2	-0.7 (-0.2%)	-1.9 (-0.6%)
Top	3	+6.7 (+2.3%)	-6.5 (-2.2%)
Vertical	1	-34.1 (-13.2%)	-20.4 (-7.3%)

Table 4.1: Difference in the mean hardness between soft roots (Plates 1 and 3) and standard (Plates 2 and 4), with percentage variation in parentheses.

4.4 SEM

As discussed in Section 4.2, the use of SEM or EBSD can be valuable in overcoming the limitations encountered with standard optical microscopy. The output from every SEM compositional analysis is presented in Figure 4.17. The data extracted was then processed into the results presented in Figure 4.18.

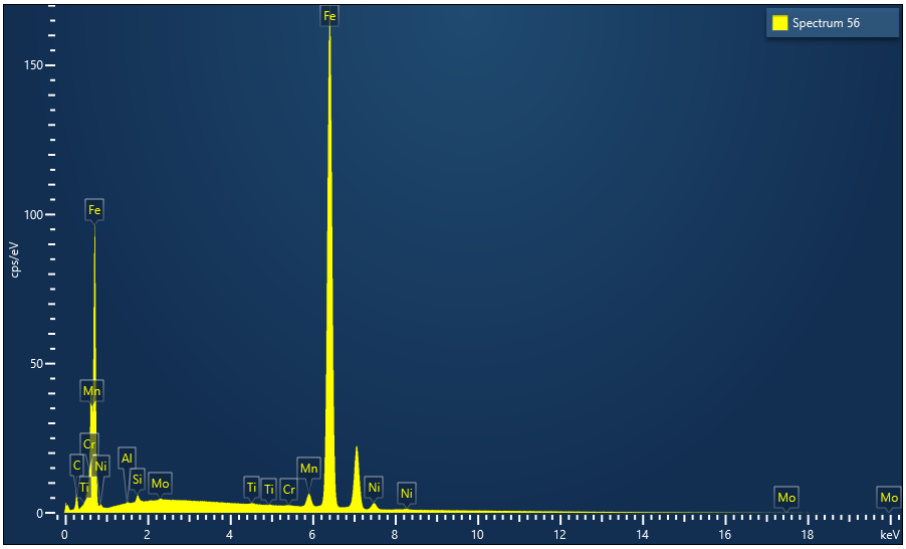

Figure 4.17: EDS spectrum showing the elemental composition

The alloying elements Ni, Mo and Cr were selected due to their important roles, as described in Table 2.1. However, since there is a significant difference in nickel content between WB 6132 (higher strength WM) and Tubrod 15.17 (lower strength WM), as shown in Table 3.4, Ni appears to be the most effective marker to illustrate dilution throughout the section. The graphs are organised to compare the corresponding locations from different weld samples (1A vs 2A, 1B vs 2B, etc.), as described in Figure 3.9. It is important to highlight the clear transition in the nickel composition, particularly in region B for samples 1 and 3, where SRT was applied.

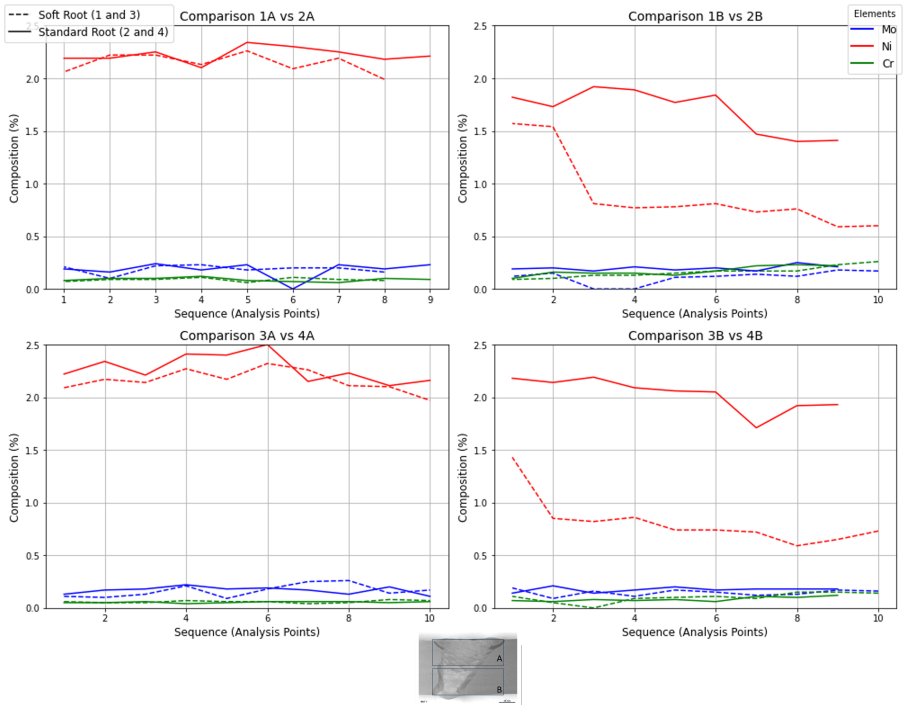

Figure 4.18: Chemical composition for Mo, Ni and Cr across welding regions

As discussed by Goldstein (28), the contrast in secondary electron (SE) images is predominantly driven by surface topography. From Figure 4.19, a difference in contrast can be observed between the SEM images of the Standard and Soft Root regions. The brightness observed in the micrographs is directly influenced by the emission of secondary electrons (Table 3.10), which is increased by the microstructural variations present on the surface.

Continuing with the SEM analysis, three key regions were chosen to visualise how the chemical composition and dilution of the joint affect the microstructural properties as described in Figure 4.20: transition between fillers (blue line), Tubrod 15.17 filler (orange line), and WB 6132 filler (green line). These locations were selected based on the height of the soft root region as explained in Section 3.4.

Figure 4.20 depicts an interesting fluctuation in nickel content which might suggest that, even though the scan runs a horizontal line, the region being analysed is not chemically uniform. Therefore, the observed gradient is probably more likely due to the fact that points 1 and 2 were parts of the weld beads in different regions. Moreover, from 3 to 4 and 5, it is clear that there is a transition from WM to BM, as the alloying content of the final observations is in accordance with Table 3.1.

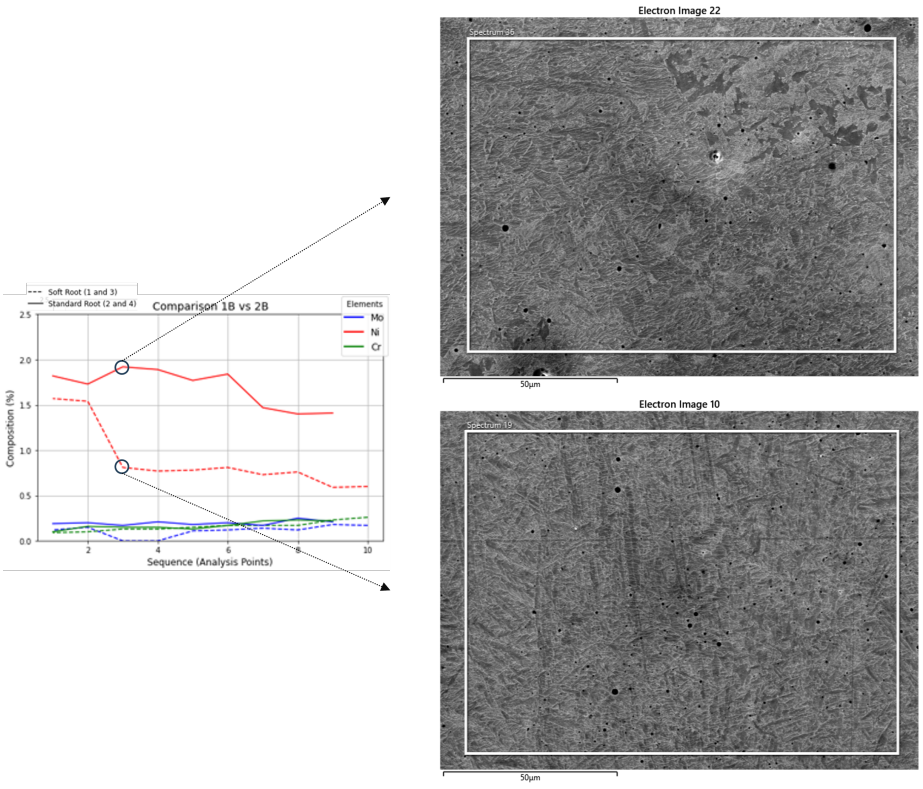

Figure 4.19: Nickel distribution and microstructural features for Plates 1 and 2

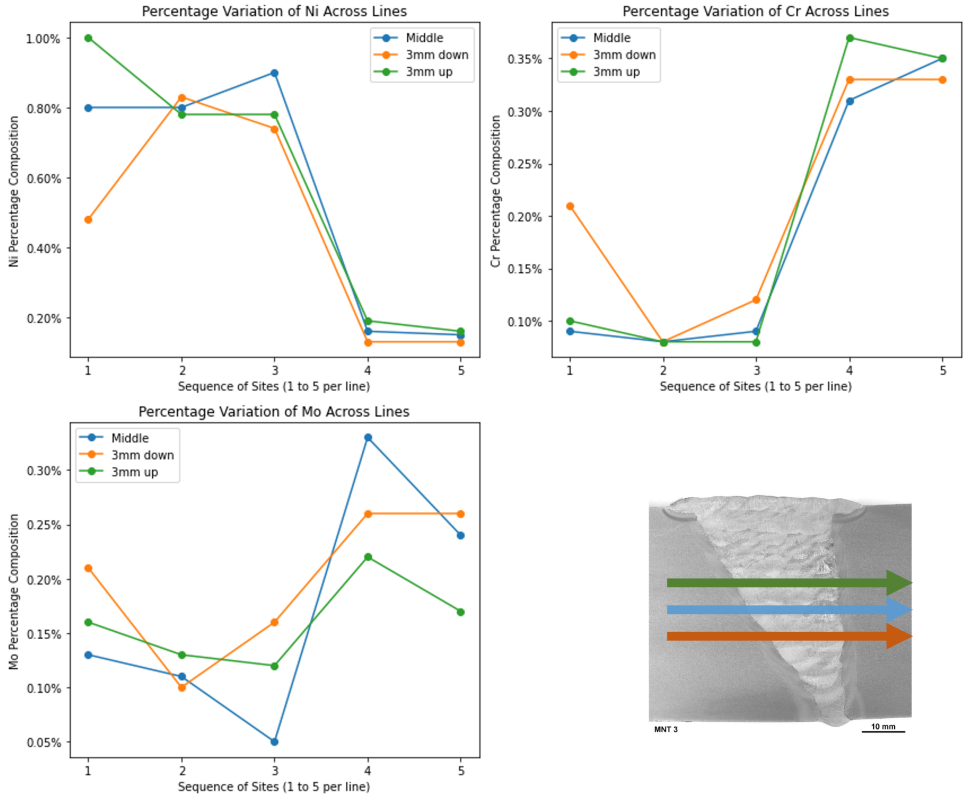

Figure 4.20: Chemical composition over horizontal lines

Further investigation can be performed by examining images with higher magnification at point 1 of graphs on Figure 4.20. In the SEM micrograph at 5000× magnification (Figure 4.21), it is already possible to notice a clear difference in topography among the three regions. The middle line, which is at the interface of the two consumables, presents the most heterogeneous appearance, as it is marked by a mixed composition where a variety of phases and grain morphologies is being developed. However, the lower line appears smoother and more uniform, highlighting the low carbon equivalent and alloying content of Tubrod 15.17. The upper line, on the other hand, shows a more textured surface, which correlates with its higher Ni and alloy content. This difference becomes even more evident in Figure 4.22, at 13000× magnification.

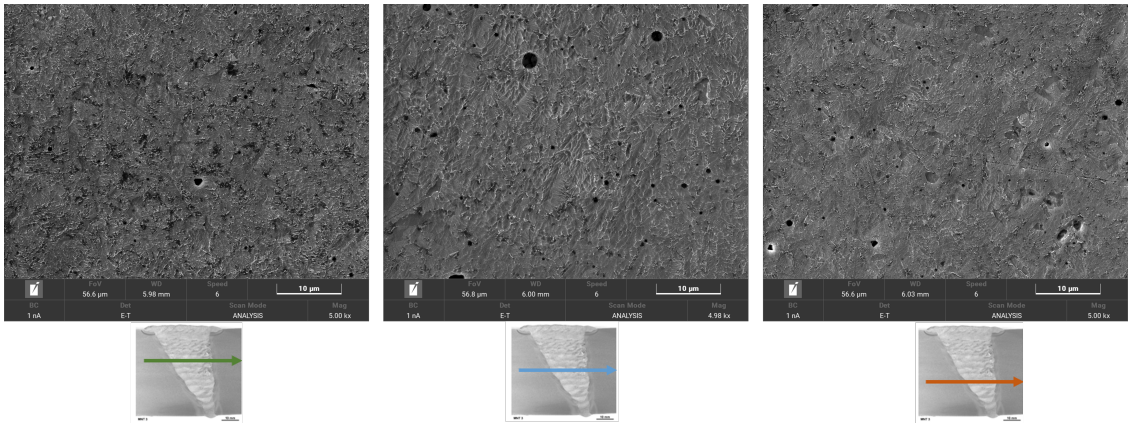

Figure 4.21: SEM images at 5000× magnification

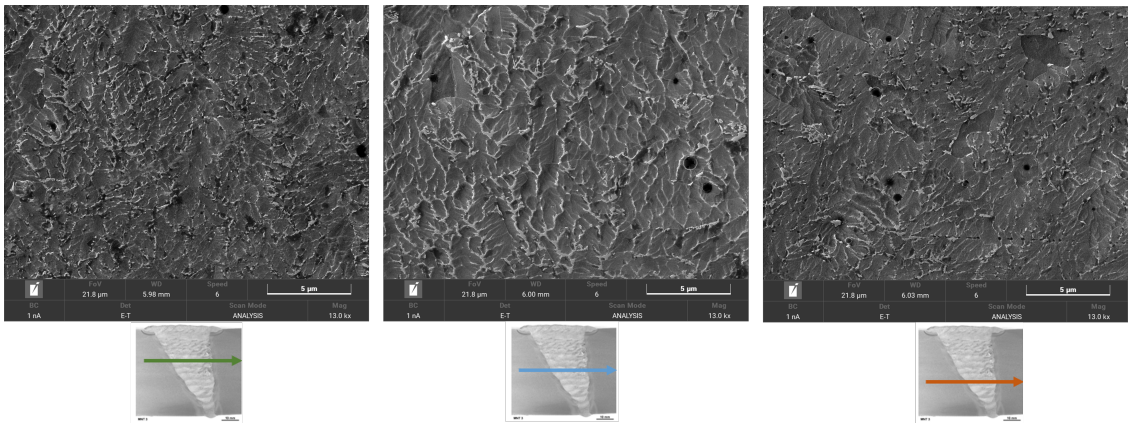

Figure 4.22: SEM images at 13000× magnification

4.5 Tensile testing

The results of the transverse tensile tests are presented in Figure 4.23. Except for sample 4B, all specimens met the minimum and maximum requirements defined in (8).

Sample 4-B, which corresponds to the root region of Plate 4 (standard root), showed a significantly lower UTS value of 633 MPa. This reduction is consistent with the defect shown in Figure 4.1, as discussed previously in Section 4.1.

A reduction in the strength of sample 1 compared to sample 2 was already expected. However, one of the main objectives of this research was to quantify this offset. The results show that this difference is relatively small, with a value of 3.5%.

For the thicker plates (3 and 4), the cap specimens (3-A and 4-A) had the best performance. These upper regions likely benefitted from the overlap of weld passes and thermal cycles during deposition, which may have contributed to microstructural refinement and improved strength.

In addition to strength, ductility was also an important outcome of this research. Table 4.2

presents evidence of elongation for all samples. This is also illustrated in Figure 4.24. Comparing Sample 1 and 2, the former, where the SRT was applied, displays a more pronounced necking and deformation before failure, suggesting greater ductility.

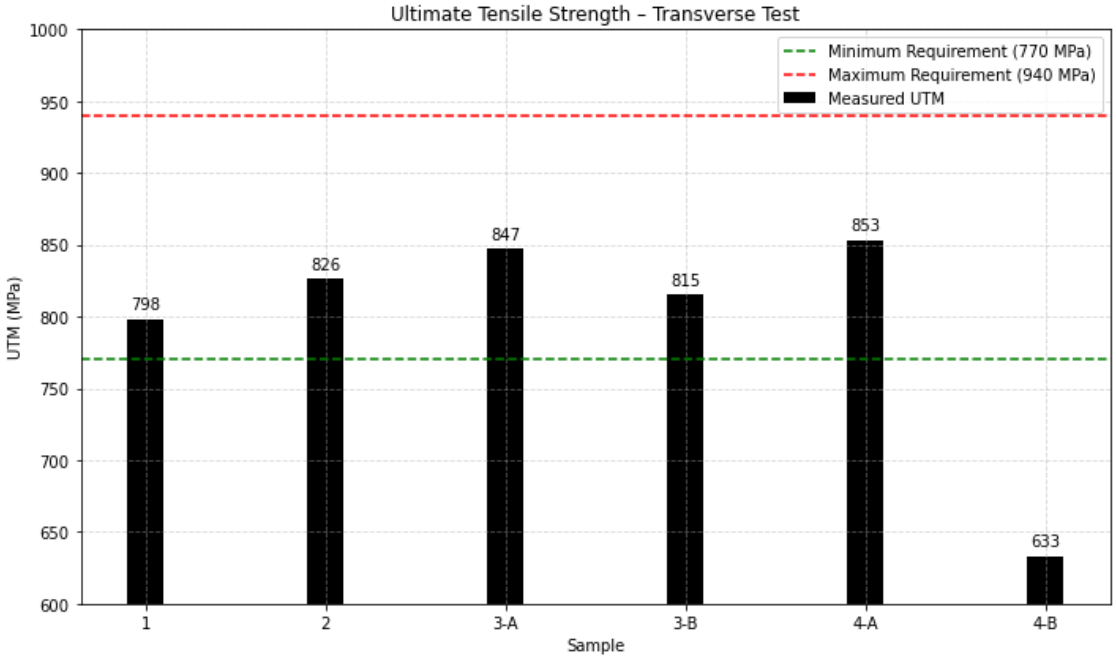

Figure 4.23: Tensile test results

Sample	Final Gauge Length (mm)	Elongation (%)
1	84.21	68.41
2	83.32	66.63
3-A	80.09	60.18
3-B	86.29	72.58
4-A	83.67	67.35
4-B	68.71	37.43

Table 4.2: Elongation results for all tensile specimens

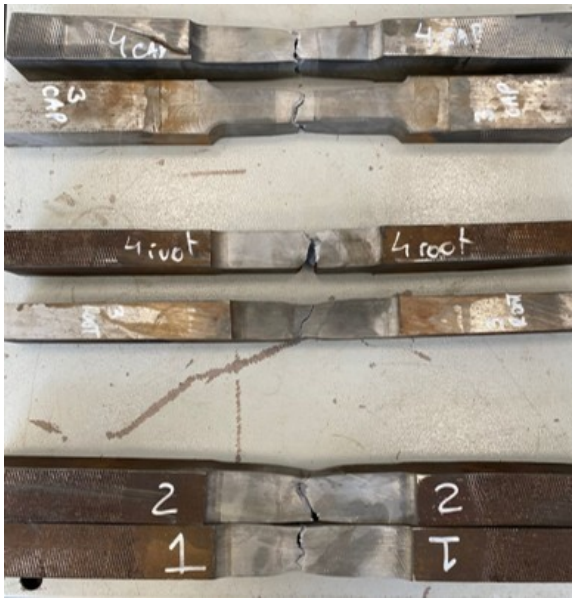

Figure 4.24: Fractured tensile specimens after testing

4.6 Impact testing

The results of the impact tests are presented in Figure 4.25 and Figure 4.26. As mentioned in Section 3.5.5, for each location, 3 samples were extracted and tested. As specified in (8), the mean value must be above the 30 J minimum requirement.

Sample 2 presents a mean value of 43 J, while sample 1 reached 56.67J, representing a 32% increase in performance. This superior performance aligns with the expected ductile behaviour of the WM.

On the other hand, for plates of higher thickness, sample 4 exhibited a lower resistance in the impact tests, which is consistent with the defect shown in Figure 4.1. Furthermore, sample 3 did not achieve the same results as sample 1, but still presented satisfactory outcomes above the minimum requirements.

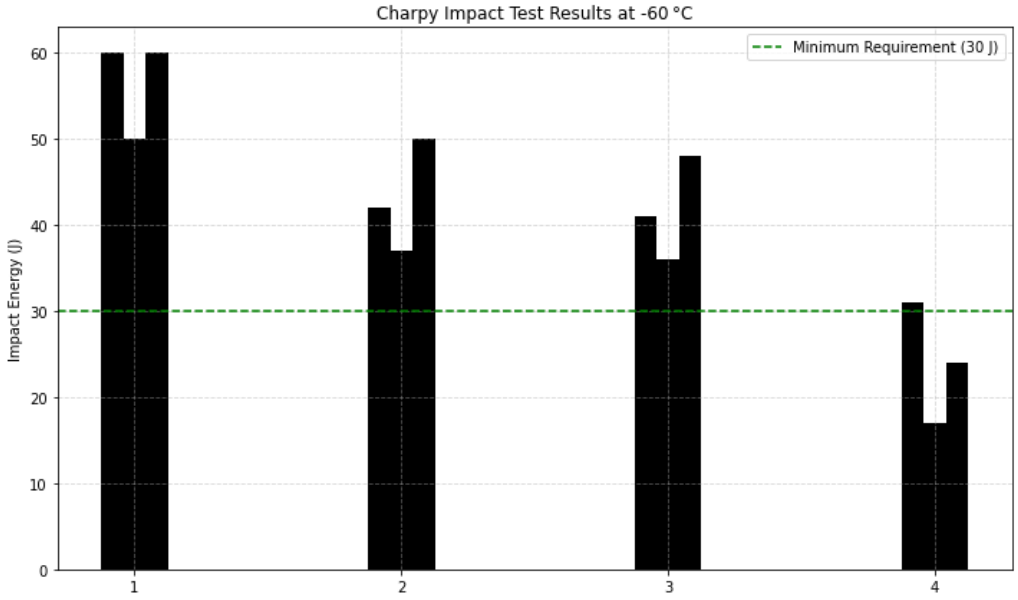

Figure 4.25: Impact tests results

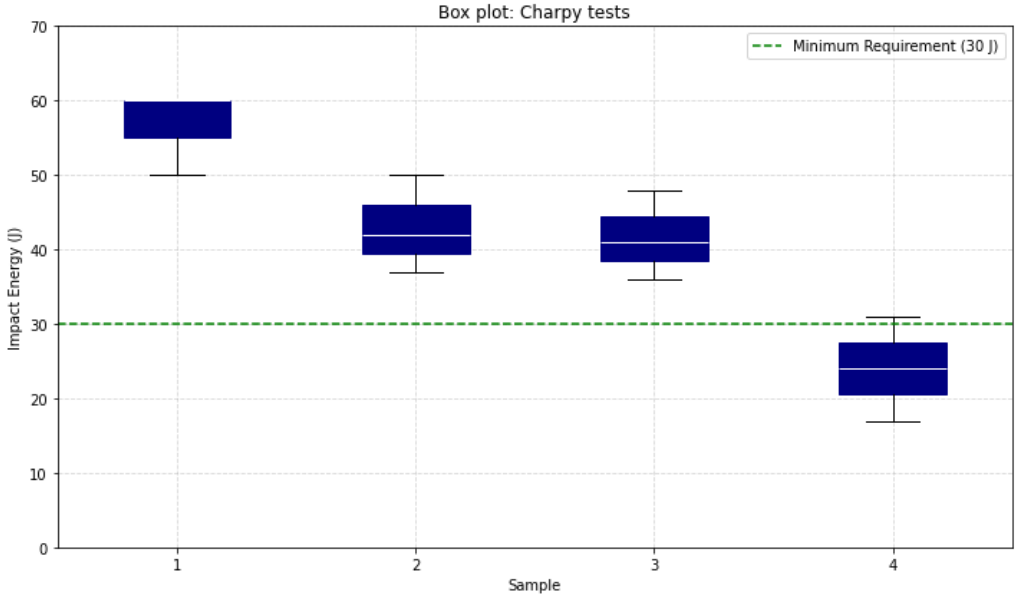

Figure 4.26: Impact tests results

Chapter 5

Discussion

Chapter 4 provided a broad view of how the techniques used in this research perform in terms of microstructural and mechanical performance. This chapter aims to examine this in depth, both by connecting these findings with the data available in the existing literature and by interpreting their implications.

5.1 Welding Mismatch and Efficiency

The concept of mismatch was addressed in Section 1.2. However, when applying an undermatching only in the root, it is still not clear whether this represents an overmatch or undermatch. Table 5.2 presents the values of mismatch ratios applied in this research for both WM used. It is worth mentioning that, unlike the BM certificates, which provide a specific UTS value, the welding consumables datasheets provide a tensile strength range. Given that, mismatch ratios were calculated in a range using the UTS range for the filler metal.

Ran et al. (29) proposed a large study on the mismatch of welding joints for high-strength steels, testing over 100 specimens within a mismatch ratio of 0.77 to 1.33. Their results are shown in Figure 5.1b. Compared with that extensive dataset, the present work is more limited in specimen number due to material and resource constraints. However, the results obtained were sufficient to capture the main trend and provide meaningful insight into the application of the SRT.

Material	**UTS (MPa)**
BM (35 mm)	856
BM (50 mm)	854
Tubrod 15.17	500–640
WB 6132	760–900

Table 5.1: UTS values

Plate	**Tubrod 15.17**	**WB 6132**
35 mm	0.58	0.89
50 mm	0.59	0.89

Table 5.2: Mismatch ratios

According to Eurocode 3 Part 1-12 (11), the EC3 curve, illustrated in Figure 5.1, represents the expected mechanical behaviour of a welded joint as a function of its mismatch ratio. There is a linear increase in performance up to a mismatch ratio of 1.0, beyond which the curve reaches a plateau. In other words, the joint strength is governed by the weaker of the two materials: BM or WM.

To plot the curve shown in Figure 5.1a, mismatch ratios were taken from Table 5.2, and normalised load values were calculated by dividing the tensile test results (Figure 4.23)

by the BM properties given in Table 3.2. Following a conservative approach, the lower bound of the WM UTS range was used.

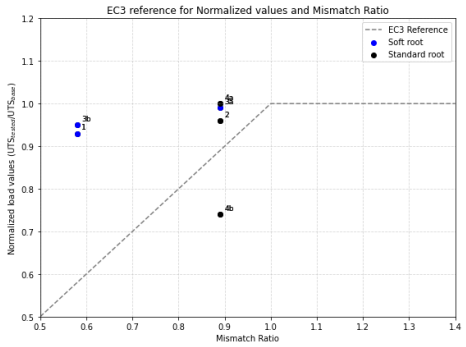

(a) Experimental results from this study

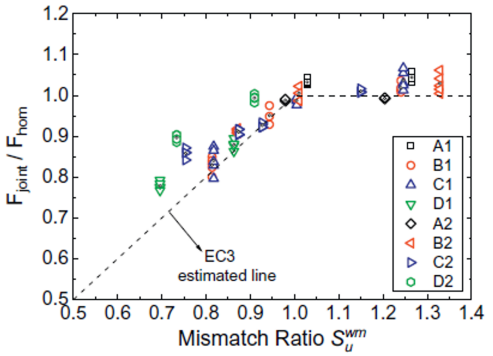

(b) Reference from Ran et al. (29)

Figure 5.1: Comparison of EC3 reference and experimental results

While the results shown in Figure 5.1b closely follow the EC3 trend, the experimental data from this study present some deviations. Samples 1 and 3b, both using SRT, lie well above the EC3 reference line, even though their mismatch ratio is considerably lower. This indicates that applying an undermatched consumable in the root does not necessarily reduce global joint performance. These samples may behave closer to a matched or even overmatched joint in practice.

It is also worth noting that, as discussed in Section 4.5, samples 3 and 4 were subdivided into cap and root regions. In the current results, samples 2, 3a, and 4a group closely around the EC3 curve, reflecting behaviour in line with theoretical expectations. In contrast, sample 4b (which corresponds to the root of Plate 4) falls significantly below the curve, reflecting the presence of a lack of fusion defect pointed out earlier.

This defect may be attributed to insufficient heat input, improper cleaning between passes, or reduced accessibility during deposition. Furthermore, it is possible that inadequate clamping allowed thermal stresses to close the joint gap prematurely, thereby limiting fusion during welding. The presence of this defect could compromise mechanical performance, as will be explored in further detail in subsequent sections.

5.2 Mechanical Performance

Figure 5.2 presents a comparison between the hardness profiles obtained in this study and another found by Mendes et al. (13). Although the graphs are based on different Vickers hardness scales—HV1 in the present work and HV10 in the literature—they provide valuable insights. First, the left-hand graph exhibits a higher degree of fluctuation, which is likely related to the increased sensitivity of the HV1 test due to its lower applied load.

Despite this, it is possible to observe that the hardness gradient in the present study is more pronounced compared to that of the literature, particularly in the WM and HAZ regions. It is also worth noting that in the referenced study a slightly undermatching filler metal (0.95

mismatch ratio) was used, which may explain the significant drop in hardness observed in the blue line of the right graph. This contrast reinforces the role of an undermatching in the root area.

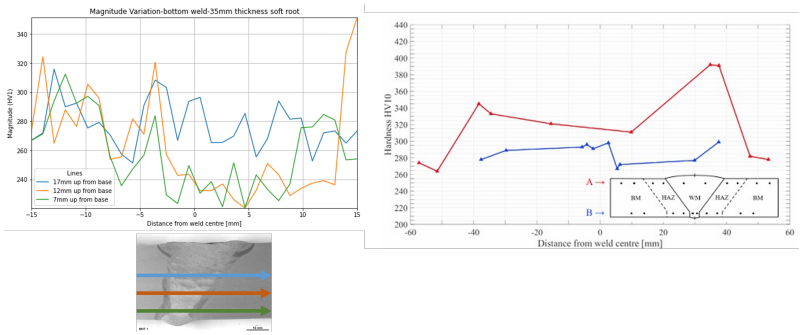

Figure 5.2: Comparison of hardness values

5.3 SRT in Literature and Comparative Context

The use of SRT in welding engineering is not new, as discussed in Chapter 2. From different angles, authors have explored the technique. In order to draw a clearer comparison, two more studies were considered alongside the present work. A summary of key information from each study is presented in Table 5.3.

Author	**BM**	**Mismatch Ratio**	**Soft Root %**	**Focus**
Rak et al. (17)	HT80	1.08 (fill) 0.76 (root) 0.57 (root)	25% / 45%	Crack propagation
Umekuni et al. (16)	HT80 HY100 HY130	0.61 (root) / 0.94 (fill) 0.83 (root) / 1.02 (fill) 0.64 (root) / 0.79 (fill)	One pass only	Pre-heating / crack initiation
This Study	S690	0.57–0.59 (root) 0.86–0.88 (fill)	24% / 34%	Mechanical performance

Table 5.3: Comparative overview of SRT welding strategies

When comparing the studies shown in Table 5.3, some interesting insights can be drawn. Firstly, although all three studies used SRT, the amount of softer filler applied varies from a single-pass root layer to as much as 45%. Despite this, none of the studies reported a significant drop in global mechanical performance, suggesting that the SRT, even when it represents a larger portion of the joint, does not necessarily compromise strength when proper procedures are followed.

Secondly, while Rak et al. (17) and Umekuni et al. (16) focused on fracture behaviour and conducted CTOD tests, this research fills a gap by presenting the overall mechanical performance associated with different proportions of soft root layers and showing how a heterogeneous WM zone behaves.

Finally, this study provides new data for a different HSS (S690), which has not been explored in previous literature. While Rak and Umekuni focused primarily on fracture mechanics, this study evaluated global mechanical behaviour. Together, the two studies and the present work suggest a consistent narrative: the SRT can be used without compromising weld strength.

5.4 Normative Gap for SRT and Undermatched Joints

From a historical point of view, it's worth noting that both studies presented in Table 5.3 were developed in the late 1990s—a time when welding HSS posed significant challenges, particularly regarding HICC. As shown in Table 3.3 and Table 3.1, the lower-strength consumable reduces the carbon equivalent (CE) by 36% compared to the WM, while the higher-strength consumable has a CE that is 135% greater than that of the lower-strength one. This clearly illustrates the metallurgical trade-off: increasing strength in the consumable typically requires more alloying, and more alloying usually means a higher CE, which raises the risk of HICC.

Using a lower-strength WM in the root offers a smart mitigation strategy. It helps to reduce both the overall CE in the joint and the resulting hardness. Still, most standards remain conservative when it comes to the use of mixed consumables in a single weld. There is little explicit guidance on the application of the SRT explored in this study.

This leaves engineers in an uncertain position when designing welding procedures for modern steels (especially HSS and above), where finding a perfectly matched consumable can be a real challenge. In practical terms, this represents a normative gap. Providing clearer tools and guidelines for welding engineers would allow for the safe implementation of more efficient and flexible strategies. Design standards should continue to evolve to meet metallurgical advancements and offer solutions that reflect real-world needs.

5.5 Summary

Finally, after following the steps described in Figure 5.3 and gathering the results from this, it is clear that SRT, even with mismatch ratios as low as 0.57, can deliver to the customer mechanical performance in accordance with requirements, provided that welding parameters are adjusted.

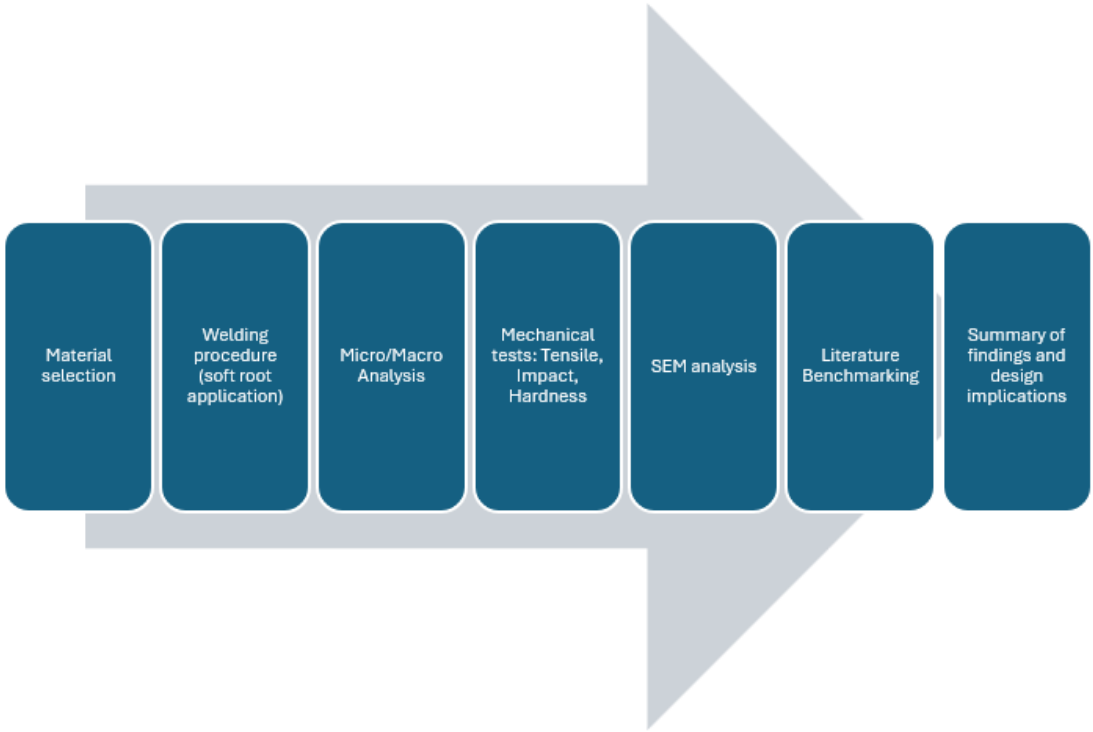

Figure 5.3: Summary workflow of Research

This study fills a gap, integrating tensile, impact, and hardness testing together with Micro, Macro and SEM analysis. This offered a comprehensive assessment of the proposed technique.

Overall, the research supports SRT as a viable and strategically useful approach for mitigating HICC risk without compromising structural integrity, especially in alloy-sensitive or design-constrained scenarios.

Chapter 6

Conclusion

6.1 Limitations

As expected for an experimental study, this research faced challenges and limitations that should be acknowledged as lessons learnt for future research. First of all, the number of specimens was limited due to constraints related to the availability of materials and personnel involved. Although the results show trends and provide insight, a larger number of samples would benefit the study as the matrix test could be expanded and a broader statistical view would be presented as it would be possible to explore the changing of more variables.

Secondly, this research focused only on two main variables: plate thickness and filler metals. Other interesting variables such as heat input variation, heat treatment, and residual stresses were not thoroughly investigated. These factors, among others, could influence weld performance and require further analysis.

Finally, despite discussions with the Eurocode (EC3) framework and other literature references, the absence of normative guidance for soft root configuration limits how the findings could be applied in design scenarios.

6.2 Summary of Findings

In this research, the mechanical performance and metallurgical implications of using a soft root configuration in high-strength steel (S690) were investigated. The study combined tensile and Charpy impact testing with hardness profiling, SEM observations, and metallographic analysis. Two filler metals were applied: a lower-strength wire for the root and a higher-strength wire for the fill and cap regions. The key findings can be summarised as follows:

- **Mechanical integrity** was not compromised by the use of a soft root, even with mismatch ratios as low as 0.57.
- **Charpy impact results** indicated a noticeable improvement in toughness and a reduction in hardness of approximately 10% when the SRT was applied. This trade-off appears to be favourable in applications where ductility is a priority.
- When compared to the **EC3 theoretical behaviour**, the soft root samples exceeded expectations, suggesting that an undermatched root does not necessarily result in an overall undermatched joint.

- A clear **normative gap** was identified, which currently discourages welding engineers from adopting soft root strategies due to the lack of explicit design guidance and code validation.

Taken together, these findings support the idea that the **SRT** can be used as a strategic and effective approach to the welding of HSS, particularly in scenarios where the risk of HICC or the limited availability of WM presents challenges, highlighting a critical technical gap that still exists in welding engineering.

6.3 Recommendations and Future Work

The observations and conclusions made in the present study allow for the evaluation of possible improvements and further investigations to enhance the SRT in the welding of HSS. Consequently, some suggestions are presented below to achieve even better results that would complement the findings of this study and the existing literature, providing a broader view of the technique.

- Perform fatigue and CTOD tests on specimens with different heights of the soft roots.
- Explore alternative consumables and different combinations, as other researchers have done. This would allow for an analysis of various mismatch ratios.
- Investigate different thermal cycles for preheating and post-weld heat treatment, and evaluate whether it is feasible to increase productivity when applying the SRT.
- Conduct finite element simulations to understand the effect of varying proportions of different WM. This approach would allow for a more accurate evaluation of parameters such as temperature distribution, residual stresses, and distortions. With these results, a more efficient test matrix could be defined, optimising both cost and time in future research.
- There is a strong potential to contribute to normative development by collecting and consolidating results from various soft root strategies and proposing technical guidance for their application. Conducting a sensitivity analysis for mismatch ratios would also be valuable in supporting the selection of appropriate filler metals.

References

1. Shi G, Hu F, Shi Y. Recent research advances of high strength steel structures and codification of design specification in China. International Journal of Steel Structures. 2014 12;14(4):873-87.

2. European Committee for Standardization. CEN, (ed.). BS EN 1993-1-8: 2004 Eurocode 3: Design of Steel Structures. CEN (EUROPEAN COMMITTEE FOR STANDARDIZATION); 2004.

3. Antonio Augusto Gorni. Desenvolvimento de Aços Alternativos aos Materiais Temperados e Revenidos com Limite de Resistência entre 600 e 800 MPa. Campinas: Universidade Estadual de Campinas; 2001.

4. Krauss G. Steels: Processing, structure, and performance. 2nd edn. ASM International; 2015.

5. Urabe T. High Formability Steel. Encyclopedia of Materials: Metals and Alloys. Elsevier; 2022. p. 3-11.

6. Christian Schneider. Influence of High Energy Density Fusion Welding Techniques on Welding of Structural Steel S960. Graz: University of Technology Graz; 2020.

7. British Standards Institute (BSI). BSI, (ed.). BS EN 10020:2000- Definition and classification of grades of steel. London: British Standards Institute; 2000. Available at: `https://bsol.bsigroup.com/`.

8. British Standard Institute (BSI). BSI, (ed.). BS EN 10025-6: Hot rolled products of structural steels. Technical delivery conditions for flat products of high yield strength structural steels in the quenched and tempered condition. London: British Standards Institute; 2022.

9. KOICHI MASUBUCHI. Analysis of Welded Structures: Residual Stresses, Distortion and their consequences. 1st edn. Oxford: Pergamon Press; 1980.

10. Alabi AA, Moore PL, Wrobel LC, Campbell JC, He W. Tensile behaviour of S690QL and S960QL under high strain rate. Journal of Constructional Steel Research. 2018 11;150:570-80.

11. EUROPEAN COMMITTEE FOR STANDARDIZATION. CEN, (ed.). EN 1993-1-12: 2007 Eurocode 3. Design of steel structures. Additional rules for the extension of EN 1993 up to steel grades S 700. Brussels: CEN (EUROPEAN COMMITTEE FOR STANDARDIZATION); 2007.

12. British Standards Institution. BSI, (ed.). UK National Annex to Eurocode 3: Design of steel structures – Part 1-12: Additional rules for the extension of EN 1993 up to steel grades S 700. London: BSI; 2008.

13. Mendes P, Monteiro M, Silva RP, Correia JAFO, de Jesus AMP, Vieira M, et al. Microstructure and Hardness Properties of a S690QL Steel Welded Joint. Procedia Structural Integrity. 2024;54:340-53.

14. J Billingham, J V Sharp, J Spurrier, P J Kigallon. Review of performance of high strength steels used offshore. Bedfordshire: Health & Safety Executive; 2003.

15. Garner J, Cosgrove T. High Strength Steels for Structural Applications: A Guide for Fabrication and Welding. London: The British Constructional Steelwork Association; 2020.

16. Koichi Masubuchi, A Umekuni. Usefulness of undermatched welds for High-Strength Steels. The Welding Research Supplement. 1997 7:256-63.

17. Inoslav Rak, Nenad Gubeljak, Zdravko Praunseis. The fracture behaviour of global/local mis-matched weld joints provided on HSLA steels. Materiali in Tehnologije. 2001;35:89-98.

18. Mochizuki M, Kawabata T. Effect of Undermatched Weld on Deformation and Brittle Fracture Behaviors in High-Tensile Strength Steel Plate Welded Joint. Volume 6: Materials and Fabrication, Parts A and B. American Society of Mechanical Engineers; 2012. p. 145-54.

19. Loureiro AJR. Effect of heat input on plastic deformation of undermatched welds. Journal of Materials Processing Technology. 2002 10;128(1-3):240-9.

20. Gubeljak N. Fracture behaviour of specimens with surface notch tip in the heat affected zone (HAZ) of strength mis-matched welded joints. International Journal of Fracture. 1999;100(2):155-67.

21. Song L, Zhang P, Li Z, Zeng J, Feng J, Su X, et al. Laser-arc hybrid welding of 25 mm high strength steel sections. Optics & Laser Technology. 2025 4;182:112193.

22. Quiroz V, Gebhardt M, Gook S, Gumenyuk A, Rethmeier M. Hot cracking in high power laser beam welding of thick high strength structural steels under restraint conditions. International Congress on Applications of Lasers & Electro-Optics. Laser Institute of America; 2010. p. 225-32.

23. Aria M, Cuccurullo C. bibliometrix : An R-tool for comprehensive science mapping analysis. Journal of Informetrics. 2017 11;11(4):959-75.

24. British Standards Institute (BSI). BSI, (ed.). BS EN ISO 17639: 2022 Destructive tests on welds in metallic materials — Macroscopic and microscopic examination of welds. London: British Standards Institute; 2022. Available at: `https://bsol.bsigroup.com/`.

25. British Standard Institute (BSI). BSI, (ed.). BS EN ISO 4136: 2022 Destructive tests on welds in metallic materials — Transverse tensile test. London: British Standards Institute; 2022. Available at: `https://bsol.bsigroup.com/`.

26. British Standard Institute (BSI). BSI, (ed.). BS EN ISO 9016: Destructive tests on welds in metallic materials — Impact tests — Test specimen location, notch orientation and examination. London: British Standard Institute; 2022.

27. Bertolo V, Jiang Q, Scholl S, Petrov RH, Hangen U, Walters C, et al. A comprehensive quantitative characterisation of the multiphase microstructure of a thick-section high strength steel. Journal of Materials Science. 2022 4;57(13):7101-26.

28. Goldstein JI, Newbury DE, Michael JR, Ritchie NWM, Scott JHJ, Joy DC. Scanning Electron Microscopy and X-Ray Microanalysis. New York, NY: Springer New York; 2018.

29. Ran MM, Sun FF, Li GQ, Kanvinde A, Wang YB, Xiao RY. Experimental study on the behavior of mismatched butt welded joints of high strength steel. Journal of Constructional Steel Research. 2019 2;153:196-208.

Chapter A

Ethical Approval Letter

11 February 2025

Dear Mr Barbosa Coutinho Freire De Souza ,

Reference: CURES/24310/2025
Project ID: 27654
Title: Application of a soft root technique to the Welding of High Strength Steels (HSS)

Thank you for your application to the Cranfield University Research Ethics System (CURES).

We are pleased to inform you your CURES application, reference CURES/24310/2025 **has been reviewed. You may now proceed with the research activities you have sought approval for.**

If you have any queries, please contact CURES Support.

We wish you every success with your project.

Regards,

CURES Team